# HPT Annex 50

## Heat Pumps in Multi-Family Buildings

## Task 4.0: Demonstration and Monitoring

## Country Report

## *AUSTRIA*

---

**Edited by** Graz University of Technology

R. Pratter, W. Lerch, R. Heimrath, R. Rieberer
Contact: rene.rieberer@tugraz.at

**September 25, 2020 (Version 1.0)**

# Contents

# Summary

The Austrian contribution within IEA HPT Annex 50 - Task 4 deals with the system description, monitoring and data analysis of a realized solar ice-storage heat pump system installed in a multifamily building with 10 apartments located in Weiz (Austria).

This report describes the system layout as well as the major components (solar collector, ice storage, heat pumps) and the measurement equipment used to monitor the system, which can operate in different modes to cover the space heating and domestic hot water demand.

After some problems in the initial phase, the system works reliably. However, the ice storage volume has been dimensioned according to the heat demands based on the buildings Energy Certificate. It turned out that the real heat demand for space heating and domestic hot water is much higher, thus the realized storage is too small leading to a direct electric heating demand in the cold season, when the storage is sub-cooled. Furthermore, the Seasonal Performance Factors (SPF) of the two differently sized heat pumps are significantly different: it ranges from 3.4 – 3.6 for the larger heat pump (design capacity 10 kW) and from 2.8 – 2.9 for the smaller one (6 kW). The overall SPF of the system (incl. the direct electrical heating demand) was about 3.1 in all monitored years (2016 – 2019).

A modification of the hardware and thus an optimization of the heating system in Weiz was not possible due to cost reasons, but the information collected in this project will help to improve the design of future ice storage systems and their hydraulic schemes.

# 1 The solar-ice storage-heat pump system in Weiz

## 1.1 Introduction

This report deals with the current state of an already installed solar-ice storage-heat pump system. The analysed system is a multifamily building which is located in Weiz (Austria). First the main components, its operating modes and the monitoring of the system are explained. The measurement data was used to analyse the current state of the system as well as to validate a simulation model (see Austrian report on IEA HPT Annex 50 – Task 3.2). The gathered knowledge have been used to identify optimization potentials and error preventions which were (partly) implemented. Finally, measurement data for the period 1/2017 – 4/2020 are presented in this report.

This report is mainly based on the Master thesis Pratter (2017) and the results of the project "Hot Ice" which was financially supported by the province of Styria (Pratter el al., 2017).

The project "Hot Ice Weiz" focused on the use of latent heat with two ice storages and two heat pumps in combination with unglazed solar collectors and a PV system. It is designed as a pilot project for local heat supply.

The construction of the MFB (multi-family building) which is located at Bärentalweg 6 in 8160 Weiz (Austria) was finished in April 2015. The building, shown in Figure 1-1, is a wood frame construction which accommodates ten different apartments on three floors. The total area adds up to 1477 $m^2$, whereof an area of 957 $m^2$ is heated. It fulfils the passive house standard and has a calculated thermal heat demand of 9.91 kWh/($m^2$a).

*Figure 1-1 Building in Weiz (Hutter, 2016)*

Figure 1-2 shows the hydraulic scheme of the heating system which is used in this building. A more detailed description of the most important components can be found in section 1.2.

As shown in Figure 1-2, the heat provided from the solar collector can either be put into the ice storage by a heat exchanger or fed to the heat pumps. It is impossible to use the heat from the solar collector directly to heat the domestic hot water (DHW) or the space heating (SH) storage because the temperature is too low and must be lifted to a higher level by the heat pumps before. Depending on the current energy demand, one or two heat pumps are in operation. The heat pumps always work in one mode (DHW or SH storage) and ensure that the temperature in the storages remains within the desired range. Instead of the solar collector, the heat pump can also use the ice storage as heat source. If both heat sources are not sufficient, it is possible to heat the two storages with an auxiliary heater. During

the summer, this system can also be used for cooling. For this, the ice storage is used directly as heat sink (“cold source"), so that no additional chiller is needed.

Furthermore, the building has a controlled ventilation system with heat recovery. With this ventilation system, it is possible to heat the supplied air. A more detailed scheme of the heating system including the sensor positions for the measurement as well as the ventilation system can be found in the Appendix.

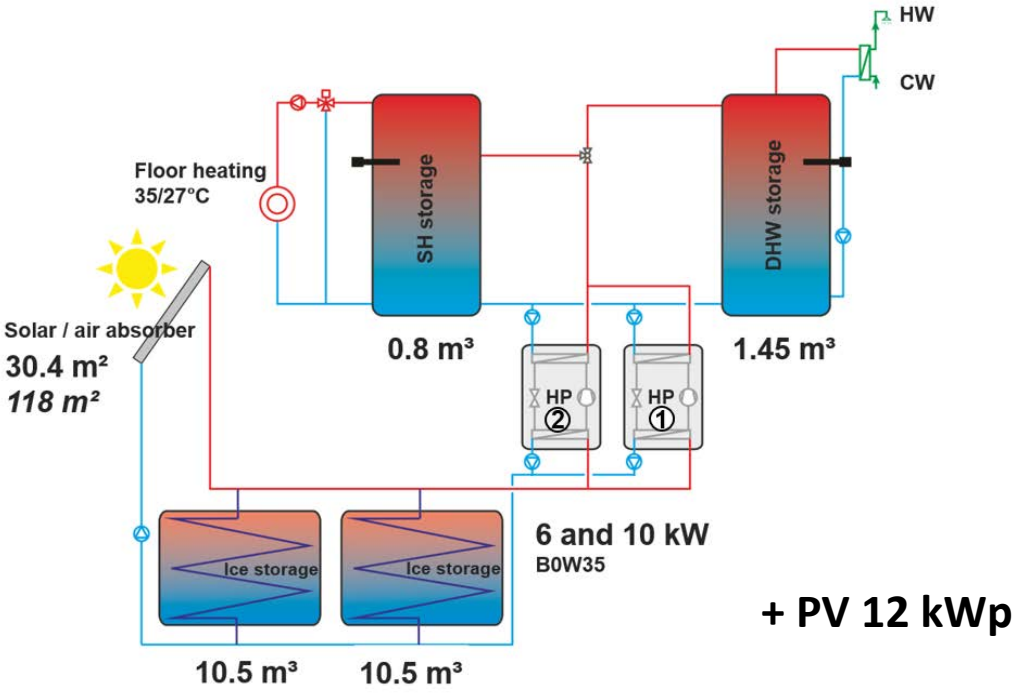


*Figure 1-2: Hydraulic scheme (Lerch, 2017)*

There are a huge number of sensors installed, which allows a detailed analysis of the functioning of the system. Some of the most important sensors are the heat meters, which measure the inlet and return temperature as well as the mass flow. In addition, they also provide the power and the heat quantity, which are calculated from the measured values and the fluid data: two for each heat pump (one for DHW and one for SH), one for the solar collector, one for cooling and one for the ventilation system. Furthermore, there are, for example sensors to measure the collector temperature, the global radiation, the ambient temperature, the electric power of the heat pumps and the electric heating elements to mention only some of them. Moreover, several sensors are installed to measure the ice storage and the surrounding soil temperatures.

The data of these sensors is not only recorded for later analysis, but can also be viewed using the HMI App (HMI-Master GmbH, 2017). This app visualizes the current system status. It is, therefore, possible to observe at any time in which operating mode the system is currently working, how high the storage temperatures are, or whether a problem occurs somewhere. In addition, all electrical and all heat quantity meters as well as the current weather data are displayed. Furthermore, the temperatures, $CO_2$ concentrations and relative humidity of each apartment are also shown. This makes the app a valuable tool for monitoring and better understanding the functioning of the system.

## 1.2 Technology description

This section is intended to provide a brief overview of the main components, such as the solar collector, the heat pumps, the SH storage, the DHW storage and, of course, the ice storages.

### 1.2.1 Solar collector

A solar collector of the type SLK F, shown in Figure 1-3, from the company “Isocal Heiz Kühlsysteme GmbH”, consisting of 13 modules is used to provide the thermal energy. It is a low temperature collector with two overlapping layers for installations on flat roofs. The whole unglazed collector is made of polyethylene (PE) without any welded or bonded joints. Further important technical data is summarized in Table 1-1.

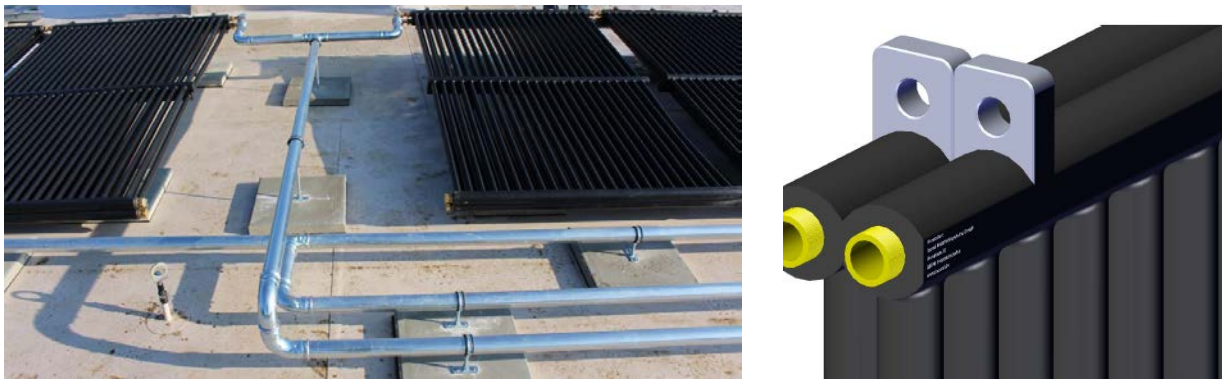

*Figure 1-3: Picture and scheme of the installed solar collector; left: HOT ICE (2017); right: Viessmann (2017)*

*Table 1-1: Technical data of one solar collector module (Viessmann, 2014)*

| **Type** | | **SLK-F** |
|---|---|---|
| Gross area | $m^2$ | 2.61 |
| Absorber area | $m^2$ | 2.34 |
| Heat exchanger surface | $m^2$ | 9.1 |
| Dimensions | mm | 2120x1225x50 |
| Weight (empty/full) | kg | 38/81 |
| Used fluid | | 35 % Ethylenglykol / Water |
| Nominal flow rate | $m^3/h$ | 0.25 |
| Maximum operating pressure | bar | 3 |
| Downtime temperature | °C | 60 |
| Hydraulic connection | | Tichelmann |

There are 13 of these modules installed, resulting in a total absorber area of 30.42 $m^2$ and a total heat exchanger surface of 118.3 $m^2$. The collector is able to use direct and diffuse radiation as well as energy from convection, precipitation and condensation.

The characteristic curve of the solar collector was not disclosed and had to be determined during the validation with TRNSYS. For details see Austrian HPT Annex 50 Task 3.2 report.

### 1.2.2 Heat pumps

To lift the heat to the required temperature level, provided by the solar collector or the ice storage, two heat pumps (connected in parallel) are used. Both are of the same type but with different capacities. Depending on the current heat demand, the heat pumps can operate together or alone but they always work in the same operating mode (SH or DHW storage). If, for example, heat pump one provides heat for the DHW storage, heat pump two can either provide heat for the same storage or stands still; i.e., it

is not possible that one heat pump provides heat for the DHW storage and the other one provides heat for the SH storage at the same time.

In the further work, the 10 kW heat pump is designated as “heat pump 1” and the 6 kW one as “heat pump 2”. Both are operating with a temperature spread of 5 Kelvin on the heat sink side (design point). For this case, the technical data is listed in Table 1-2.

*Table 1-2: Technical Data of the heat pump (Viessmann, 2015)*

| **Type BW 301.A.** | | **10 (“Heat Pump 1”)** | **06 (“Heat Pump 2”)** |
|---|---|---|---|
| *Performance data (5K spread) B0W35* | | | |
| Nominal heat output | kW | 10.06 | 5.94 |
| Cooling capacity | kW | 8.08 | 4.71 |
| Electric power consumption | kW | 2.13 | 1.32 |
| Coefficient of performance (COP) | - | 4.72 | 4.51 |
| Refrigerant | - | R410A | R410A |
| *Brine (primary circuit, heat source)* | | | |
| Contents | l | 4.0 | 3.0 |
| Min. volume flow rate (5K spread) | l/h | 1470 | 860 |
| Max. inlet temperature | °C | 25 | 25 |
| Min. inlet temperature | °C | -5 | -5 |
| Medium | | 35 % Ethylenglycol / Water | |
| *Water (secondary circuit, heat sink)* | | | |
| Contents | l | 3.4 | 2.4 |
| Min. volume flow rate (5K spread) | l/h | 880 | 520 |
| Max. inlet temperature | °C | 60 | 60 |

### 1.2.3 Space heating storage

One storage with a volume of 0.8 $m^3$ is installed to ensure the required amount of hot water for the space heating (SH). The temperature of this storage is kept between 30 °C and 35 °C. The energy, therefore, is provided from the heat pumps. In addition, an auxiliary heater with an electric power of 2.5 kW is integrated for the case that the heat pumps could not provide enough energy to keep the temperature level.

### 1.2.4 Domestic hot water storage

The domestic hot water (DHW) storage, with a volume of 1.45 $m^3$ is similar to the SH storage, however, higher temperatures of 55-60 °C are required. Moreover, an auxiliary heater with an electric power of 10 kW is integrated in this storage.

### 1.2.5 Ice storage

The heart of the whole system is the ice storage or better the two ice storages shown in Figure 1-4. Both are identical with the small difference that ice storage one is monitored more extensively because the controller uses ice storage one as input for the control and expects that the other one has the same state. They are non-insulated water filled steel-reinforced concrete containers, which are buried in the soil. To obtain an optimal heat output from the soil, care must be taken to ensure certain minimum distances between the reservoirs and the building of at least 3 m. In this case, the storages are placed with a distance of 3 m to each other and with 4 m to the cellar.

*Figure 1-4: Pictures of the ice storage in Weiz (HOT ICE, 2017)*

The freezing of the storage, indicated in Figure 1-5 by “Einfrieren”, takes place from the inside outwards and from the bottom upwards, to allow an expansion of the ice without destruction. The water filling of the reservoir is about 90% of the total volume. It is also important that the design of the cistern allows the utilization of heat from the surrounding soil. (Minder et al., 2014)

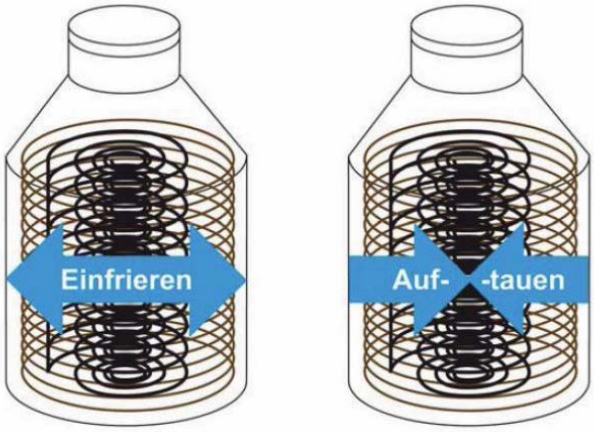


*Figure 1-5: Freezing and unfreezing of the ice storage (Viessmann, 2017)*

The basic data is shown Table 1-3.

*Table 1-3: Technical data of the ice storage (Viessmann, 2014)*

| **Type** | | **SE 12_10 B** |
|---|---|---|
| Intern volume | $m^3$ | 10.5 |
| Dimensions | m | Ø 2.7 x 3.375 |
| Weight (empty) | kg | ca. 9000 |
| Used fluid (storage medium) | | Water |
| Heat transfer fluid | | 35 % Ethylenglykol / Water |

Figure 1-6 shows the positioning of the sensors in and around the ice storages. As already mentioned, ice storage one is better monitored because it is used for the control. The sensors T_soil_1/1, T_soil_1/5 and T_soil_2/2 are positioned in a distance of one metre to the ice storages, while the others are placed without a gap. All sensors except of sensor T_soil_1/3 are installed with a thermowell. Except of that the sensor T_soil_1/3 is from the same type. Moreover all these soil temperature sensors are in the middle (height) of the ice storage.

Furthermore, there are some sensors which are installed directly in the ice storages. The sensor $T_{ice}$ is the one which is used for the control, the others are used for information purpose.

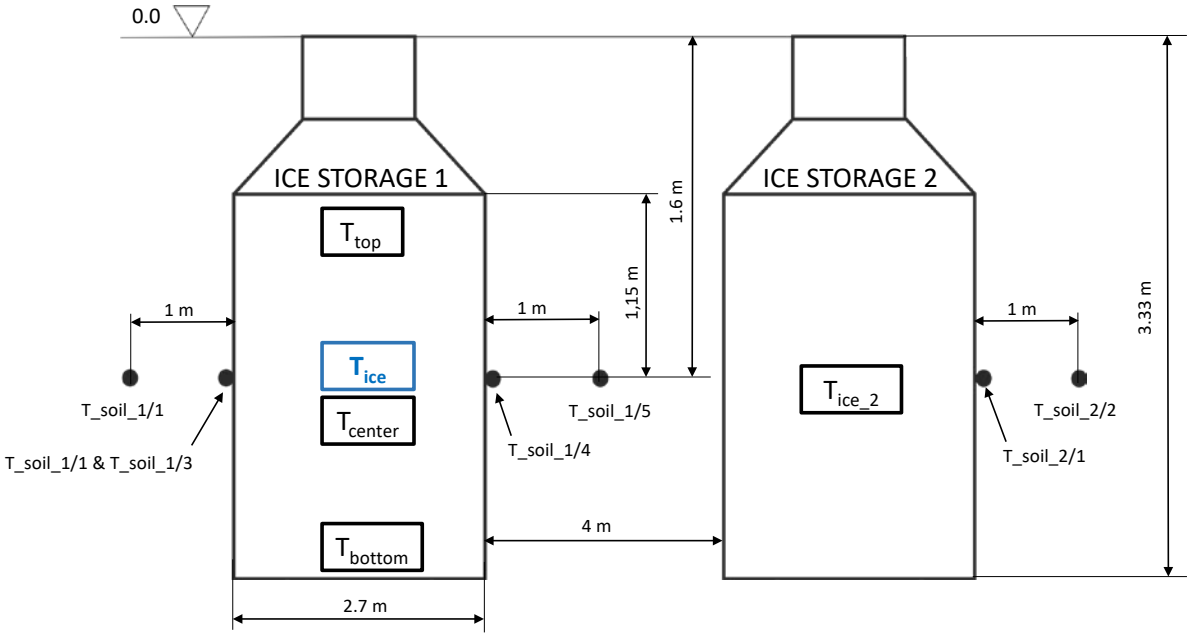


*Figure 1-6: Ice storage (Viessmann, 2017*

## 1.3 Used measurement equipment

As mentioned above, in addition to the already discussed sensors of the ice storage, a significant number of other sensors has been installed to analyse the functioning of the system. The measurement data is recorded using a KNX network that transfers the measured values to an HMI interface. This HMI App visualizes the current system status. It is, therefore, possible to access the current measured values at any time. Furthermore, all recorded data are automatically transferred to a database and can be exported as csv-file. (Hackl, 2016)

The sensor data is based on the Bachelor thesis "Analyse einer realen Eisspeicher Wärmepumpenanlage mit Solar Luftkollektoren" (Hackl, 2016). A detailed scheme of the sensors for the measurement can be found in the Appendix - Figure A- 1.

**Apartments:**

In each of the 10 apartments are KNX AQS/TH indoor sensors (Elsner Elektronik, 2017c) installed, which are used for the control of the heating and ventilation systems. These sensors measure:

- $CO_2$ concentration: Measurement range 0 . . . 2000 ppm, max. error ±50 ppm
- Temperature: Measurement range -10 . . . +50 °C, max. error ±0.4 K
- Air humidity: Measurement range 0 . . . 95 %, max. error ±5 %

Additionally, in every room a KNX TH-UP Thermo–Hygrometer (Elsner Elektronik, 2017b) is installed, which measures the temperature and the relative humidity.

- Temperature: Measurement range 0 . . . +50 °C, Accuracy ±0.5 °C
- Air humidity: Measurement range 0 . . . 100 %, Accuracy ±5 %

**Temperature:**

For the measurement of the temperatures at the energy counters, PT500 temperature sensors are used according to EN 60751.

**Electrical power:**

The energy module EM/S 3.16.1 of ABB i-bus® KNX (ABB i-bus®, 2017) is used for the measurement of electrical power.

- Effective power: Measurement range 5.7 . . . 4600 W, max. error ±6 %

The measurement power values are summed with the energy counter EMU Professional 3/75 to the meter reading.

**Weather conditions:**

On the roof of the building the weather station P03/3 - RS485 (Elsner Elektronik, 2017d) provides the values for:

- Brightness: Measurement range 0 . . .99000 Lux, max. error ±35 %
- Wind velocity: Measurement range 0 . . . 70 m/s, max. error ±25 %
- Temperature Measurement range -40 . . . +80 °C, max. error ±1.5 °C

To measure the global radiation, a KNX PY Pyranometer (Elsner Elektronik, 2017a) is used.

- Global radiation: Measurement range 0 . . . 2500 W/m$^2$, max. error ±15 %

**Heat quantity**

There are three different types of heat quantity meters installed. At the heat pumps and for the ventilation in total, five heat quantity meters of the type UH50_1,5_OEM (Siemens AG, 2017) are used (“Zähler” 1, 2, 3, 4 and 6 in the measurement scheme in the appendix).

- Heat quantity meter: Measurement range 0 . . . 150 °C, max. error 2 %

For cooling, the type “Ultraschall Sharky Heat 775” (Diehl Metering, 2017) with the same measurement range and accuracy is used (see “Zähler 5” in the measurement scheme in the Appendix). For the solar circuit, a new heat quantity meter (“Zähler Solar” in the measurement scheme) has been installed in November 2016. According to an email request, this should be of the type T550 Ultraheat (Landis+Gyr, 2017)

## 1.4 Operating modes

At the moment, the system works in four (five) different operating modes. In this subchapter, it will be clarified when which mode is used and how they work. It is also possible that the “Heat pump with ice storage mode” and the “Ice storage regeneration” work at the same time. This can be considered as a fifth operating mode.

### 1.4.1 Heat pump with solar collector mode

This mode is used when the collector temperature is higher than the ambient temperature, which is normally the case when the sun shines. Moreover, an energy demand for the SH or the DHW storage must be needed. In addition, the collector temperature must be between -4 °C and 25 °C, or if it is below -4 °C, it must be higher than the ice storage temperature. If all the requirements are fulfilled, the system works in the “Heat pump with solar collector mode”, which is illustrated in Figure 1-7.

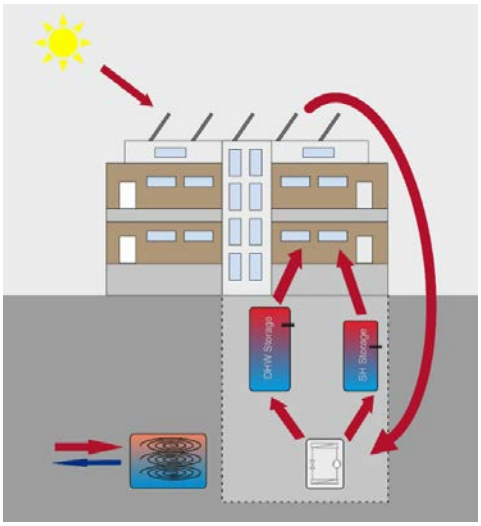


*Figure 1-7: Heat pump with solar collector mode*

This means that the energy is delivered directly from the solar collector to the heat pump. The ice storage is not used in this mode. However, if the ice storage temperature is lower than the soil temperature, the ice storage is regenerating in the meantime.

### 1.4.2 Heat pump with air absorber mode

This operation mode, shown in Figure 1-8, is similar to the “Heat pump with solar collector mode” with the difference that the ambient temperature is higher than the collector temperature, which is usually the case, when no sun shines. As already described, the installed collector is able to use diffuse radiation as well as the energy from convection, precipitation and condensation. Therefore, energy from the collector can be provided even without direct solar radiation.

For the controller, it makes no difference which of the two modes occur, however, for the validation of the simulation model these two cases must be analysed separately (see Austrian report on HPT Annex 50 – Task 3.2). For this reason, the differentiation is also done here.

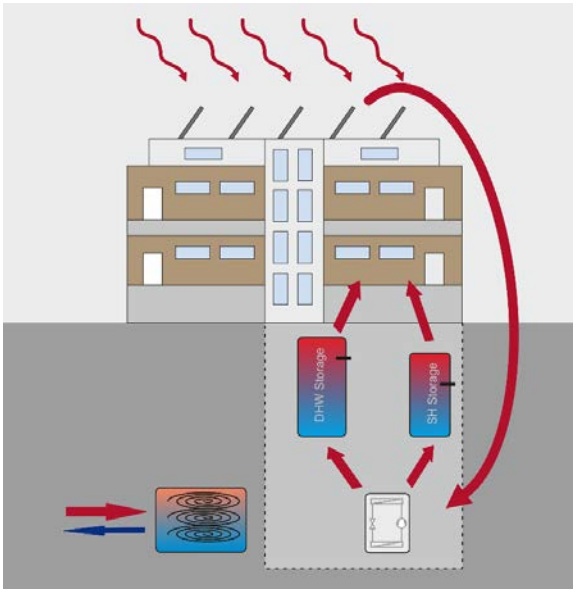


*Figure 1-8: Heat pump with air absorber mode*

### 1.4.3 Heat pump with ice storage mode

In contrast to the two previous described operating modes, the ice storage is used as the source for the HP instead of the solar collector. This is the case when the collector temperature drops below -4 °C, and the ice storage temperature is higher than the collector temperature, and if the collector temperature is higher than 25 °C. Moreover, an energy demand for the SH or the DHW storage must exist. The functionality of this operating mode is visualized in Figure 1-9.

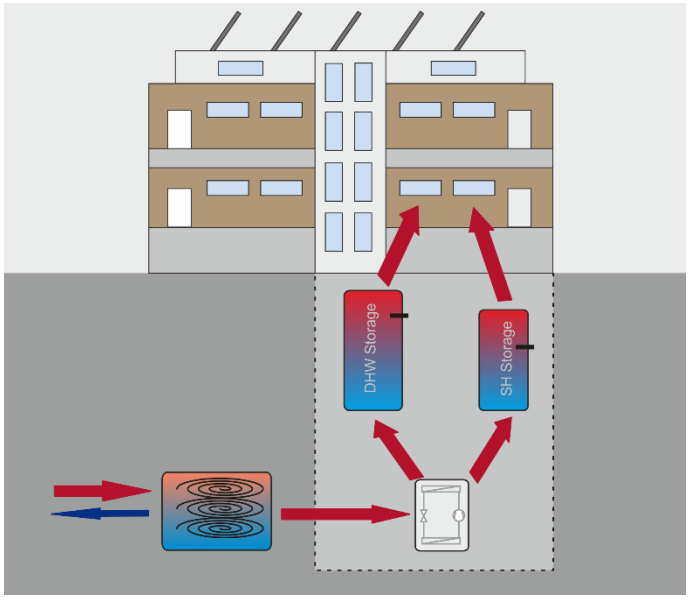


*Figure 1-9: Heat pump with ice storage mode*

### 1.4.4 Ice storage regeneration mode

The operation shown in Figure 1-10 is the ice storage regeneration mode. Neither an energy demand for the SH- nor for the DHW storage exist. In addition, the collector temperature must be higher than the ice storage temperature because the regeneration works directly without the use of the heat pumps. Moreover, the regeneration stops when the ice storage temperature exceeds 15 °C or the collector is used as source for the heat pumps.

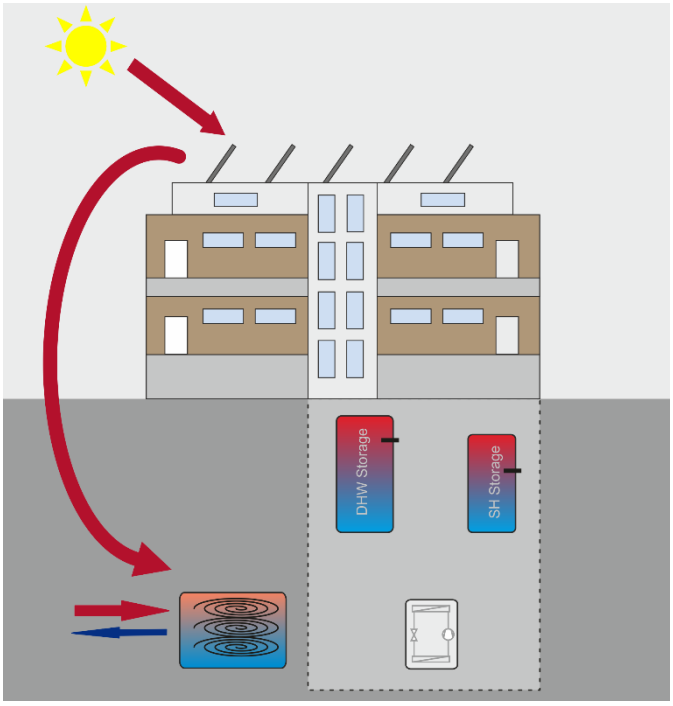


*Figure 1-10: Ice storage regeneration mode*

### 1.4.5 Combination of modes "Heat pump with ice storage" and "Ice storage regeneration"

The combination of these two modes (see sections 1.4.3 and 1.4.4) is only used when the collector temperature exceeds the maximum permissible temperature of 25° C. Moreover, there must be an energy demand for the SH or the DHW storage and the maximum temperature of the ice storage of 15 °C must not be exceeded. If this is the case, the solar collector regenerates the ice storage while the ice storage is used as source for the HP at the same time. According to these prerequisites, this operating mode occurs mainly during the summer. Figure 1-11 shows the energy flows for this case.

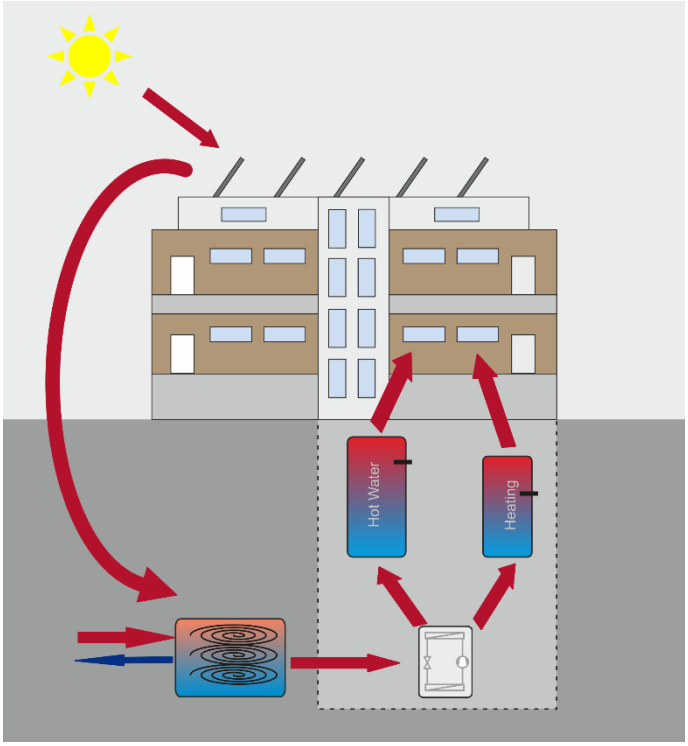


*Figure 1-11: Combined mode*

# 2 Analysis of the measurement data 2016

Basically, the data recording in Weiz has been started in July 2015. However, in the first few months some problems occurred which resulted in the fact, that for a meaningful assessment of the actual state of the system the measured data of the installed sensors are only available since February 2016. Therefore, the first measuring period was defined from February 2016 until the end of January 2017. Most of the time the data is measured in 15 min steps but there are some measuring periods with a step width of 1 min. The lower step width was necessary for the validation of some TRNSYS (Trnsys, 2011) models.

## 2.1 Limitations of the measured data

Due to data losses, system modifications and defect sensors, the data must be treated and analyzed with caution. The most important of these limitations and their effects are described here.

### 2.1.1 Data losses

During the analyzed measurement period from 01.02.2016 until 31.01.2017, some longer data failures have occurred. They happened at:

- 07.02-10.02.2016: Data losses of the whole system
- 03.05-13.05.2016: Data losses of the whole system
- 26.07-13.09.2016: Data losses of the solar heat meter
- 19.10-24.10.2016: Data losses of the whole system
- 11.11-23.11.2016: Data losses of the solar heat meter
- 10.12-13.12.2016: Data losses of the whole system

The data losses of the whole system were caused by problems with the data transmission. That means that the sensors worked correctly during this time. This differentiation is particularly important for the heat quantity of the heat meters. The fact that the sensors worked correctly during this time means that the heat quantities are known without losses for the (monthly) energy balances. An exception of this is the solar heat meter, which is explained in chapter *2.1.2 The solar heat meter* and the electric meters of the heat pumps, which is explained in chapter *2.1.3 The electric meters.*

In addition, it happens sometimes that single measured values are missing. These short data losses, however, are in a range that it has no substantial influence on the further data evaluation.

### 2.1.2 The solar heat meter

The solar heat meter is one of the most important data suppliers for the system analysis, unfortunately, however, it is one of the components that has created the biggest problems. Firstly, the solar heat meter was installed later than the other measurement devices. Therefore, these measured values have only been available since 14.12.2015. In the first time of the measurement, however, the problem occurred that the heat meter could not measure temperatures below 0 °C. As soon as negative temperatures occurred, it came to an overflow. Since the flow and the return flow temperatures in winter are often below 0 °C (collector used as source for the heat pump), the measurement data cannot be used for the preparation of the energy balance until the problem was solved on 18.01.2016.

A further problem occurred in the measurement of the thermal power delivered by the collector. Apart from the fact that no reasonable values were measured till 18.01.2016, the problem with temperatures below 0 °C still remains here. As shown in Figure 2-1, the values of the solar collector power are not plausible in case of negative temperature values.

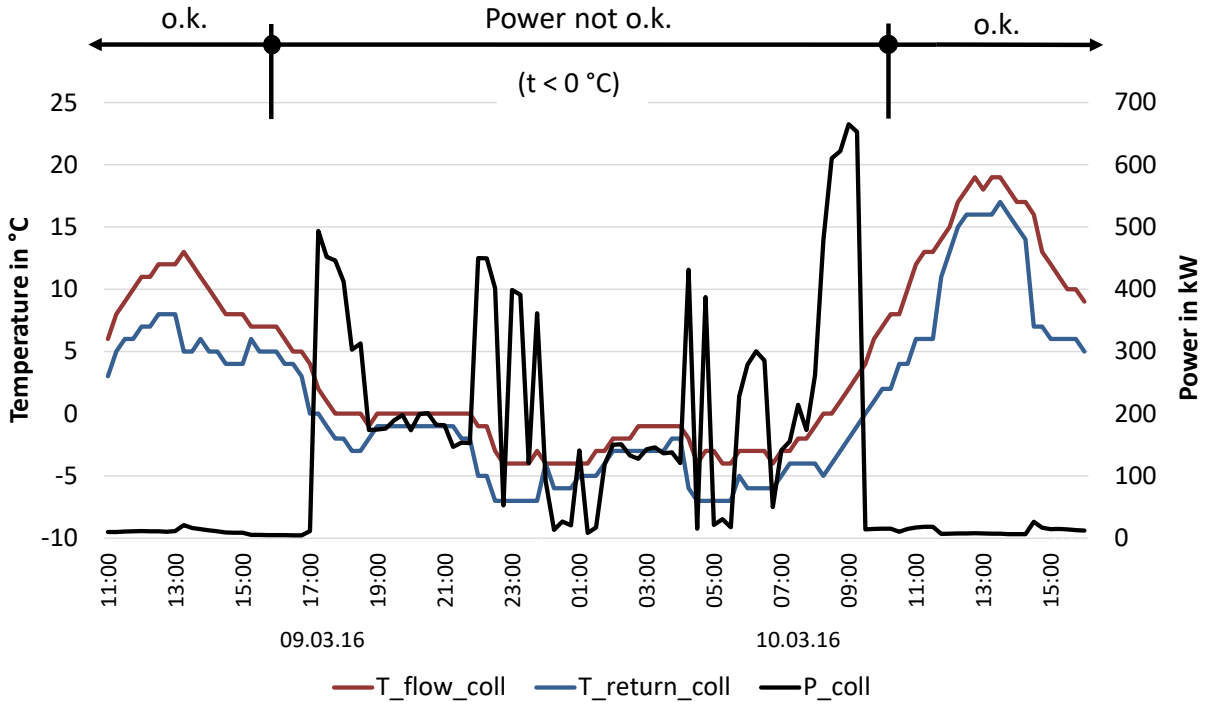


*Figure 2-1: Solar collector heat meter – temperatures & thermal power*

Due to the fact that the heat meter calculates the heat quantity using a wrong power, the heat quantity is also wrong and cannot be used for the system evaluation.

In November 2016, after some unsuccessful attempts to solve the problem, the solar heat meter was replaced by a new one. Since then, all measured values have been recorded correctly.

### 2.1.3 The electric meters

At first, the electric meters of the heat pumps and of the electric heating elements worked in such a way that the values were only updated when the data were retrieved manually. These are the jumps in Figure 2-2. Moreover, it is shown that the electric meter of the heat pump 2 did not work at all for a long period (until December 2016). It is certainly possible to calculate the values manually from the electric power, however, one should keep in mind that in this case the electric energy during the data losses cannot be considered. This is especially important in the monthly energy balances, when the different energies are partly calculated from the electric power and partly provided by the heat quantity meters.

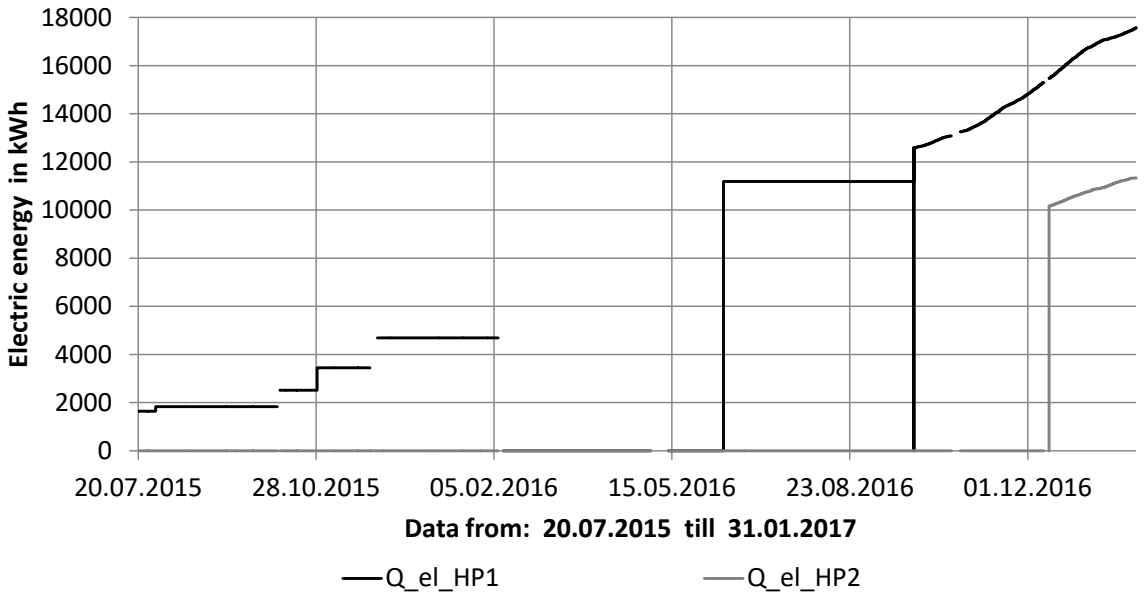


*Figure 2-2: Electric energy consumption of the heat pumps*

Since October 2016, the electric meter of the heat pump 1 has been updated and has been working correctly. The heat meter of heat pump 2 was not working until the middle of December 2016.

### 2.1.4 Conclusion

As seen from the described problems, care must be taken in using the right data for the system analysis. In addition, it has to be mentioned that at the beginning of the measurements further errors at other sensors occurred. Therefore, and especially because of the solar heat meter, a reasonable monthly energy balance can only be created from February 2016 onwards. And even from this point on, some restrictions must be made, as the measurement data failures in February and May 2016, or the intermediate removal of the solar heat meter shows.

## 2.2 Ice storage and soil temperature profile

A closer look on the ice storage temperature profile (compare Figure 1-6), shown in Figure 2-3, is a good way to get a first overview of the functioning of the system. After a settling time, the ice storage temperature was nearly constant at the adjusted maximum temperature of 15 °C (09.2015). At the end of November 2015, the ice storage temperature finally dropped down and started to fluctuate in a greater extent. The ice storage was used as source for the heat pumps but in contrast to the summer months, there was not enough energy to heat it again immediately after use. Furthermore, energy was needed for SH as well because of the start of the heating period. This can be seen in the fact that the temperature dropped relatively steeply. When the temperature increased again, the system was in regeneration mode and the ice storage was reheated by the solar collector.

However, in this period the ice storage is not used as a latent heat storage because the temperature is always higher than 0 °C. This happened for the first time in the beginning of January 2015. In Figure 2-4, this is shown in more detail. Two cold periods occurred with ambient air temperatures down to -10 °C. During the first cold period (30.12.2015 until 06.01.2016), the ice storage temperature dropped down to 0 °C for the first time and the water in the ice storage started with the phase change. For several days the storage worked as a latent heat storage. This corresponds to the planned/desired operating behaviour. At the beginning of the following second cold period (13.01.2016), however, the entire

storage was already frozen. This can be seen in the fact that the storage temperature began to fall below 0 °C. In this section, the storage temperature dropped down till -12 °C until the storage slowly began to regenerate at the end of the cold period. The subsidence of the temperature into such a low range has the effect that the desired temperature level for the heat pump can no longer be provided. The result is that the auxiliary heater must be used until the ice storage warms up again. After this period (28.01.2016), the ice storage temperature remained in the range around 0 °C so that the storage operated as latent storage again. At the end of the heating season, it finally increased to the maximum storage temperature of 15 °C which was retained during the summer.

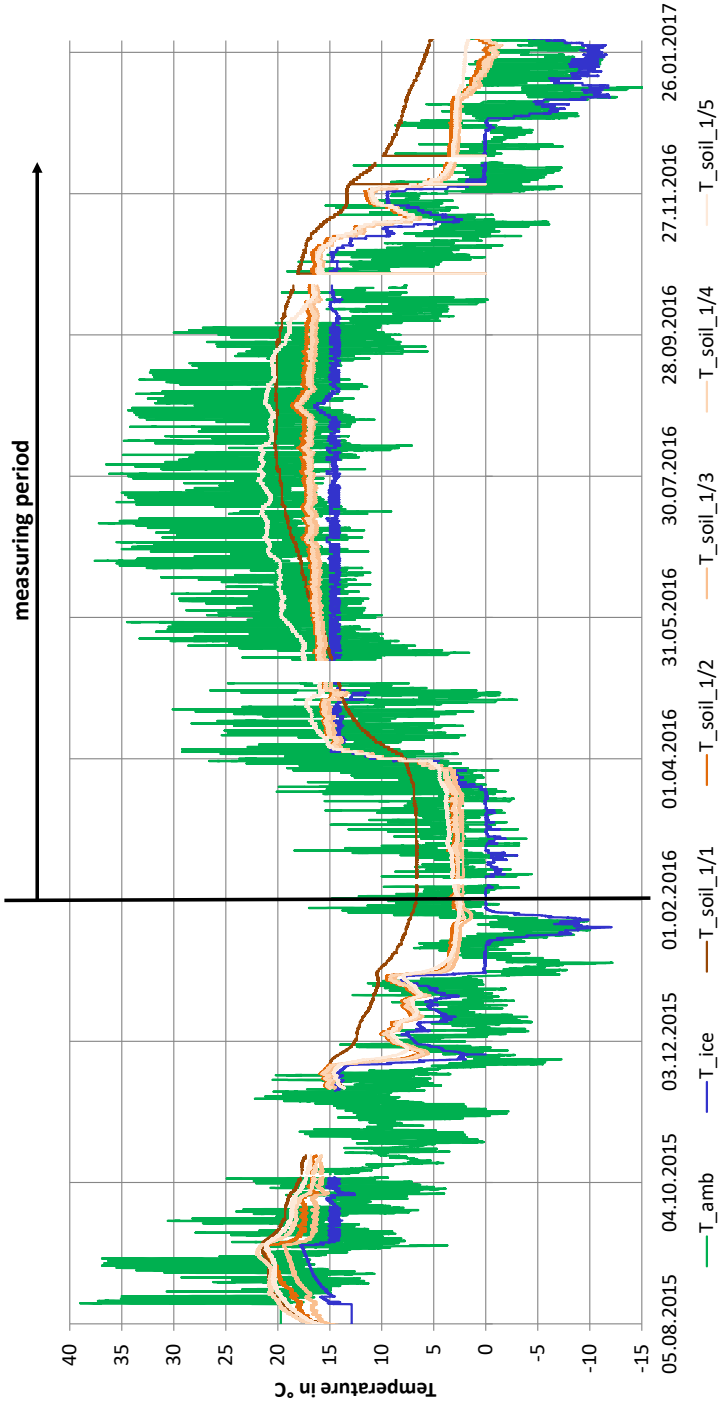


*Figure 2-3: Ice storage and soil temperatures*

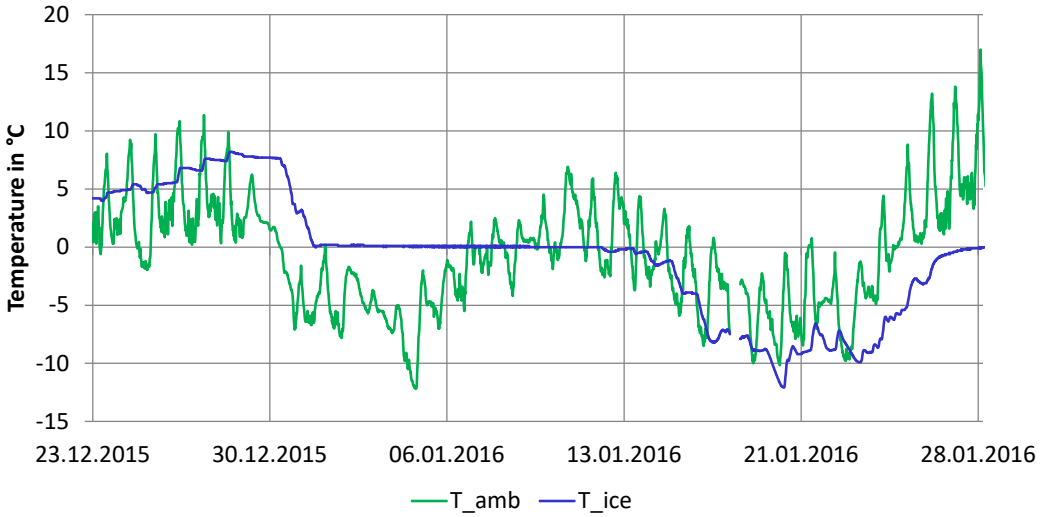


*Figure 2-4: Temperature profile of the ambient air and the ice storage*

After this, the cycle just described repeated itself, since no significant changes were made at the system in the meantime. However, the freezing of the ice storage in the second winter started earlier (28.12.2016) than in the first one. This is mainly because the winter in 2016/17 was colder. The reason that the soil around such systems is often a bit colder from the second year on, can have an influence on that though.

In addition, Figure 2-3 shows the soil temperatures around the ice storage 1. The soil temperatures are almost always higher than the ice storage temperature. This means that most of the time the ice storage gains energy from the environment instead of losing it, as most other kinds of storages do. This is one of the essential advantages of this storages, and confirms the usefulness of burying them in the ground.

A look at the individual temperatures shows that, maybe except of temperature T_Soil_1/1, although they follow the same trend they deviate from each other in their absolute values. On the one hand, this is because there are different kinds of sensors in use and on the other hand, the positioning plays an important role. These facts are shown in Figure 1-6. It is noticeable that especially sensor 1/1 deviates from the others. This one is positioned with a distance of 1 m to the ice storage on the side directed to the undisturbed soil. Particularly during the winter, the data of this sensor shows that the soil, almost unaffected by the ice storage, is much warmer than the storage. In general, it can be said that the soil temperature at a depth of about 10 m is constant at about 10 °C all year round (compare Benkert et al., 2000). In this case, the temperature fluctuates between 7 and 20 °C over the year and is not constant, because the storage is not so deeply buried and the ground temperature at a distance of one meter is influenced by the ice storage. Nevertheless, it can be seen that this temperature has the lowest fluctuation of all measured values and reacts more slowly to changes of both, the ice storage and the ambient temperature.

It is interesting to compare soil temperature 1/1 with soil temperature 1/5. Both are thermowell sensors placed with a distance of 1 m to the storage but with the difference that sensor 1/5 is on the side directed to the second ice storage. While in the summer the difference is not so big, the two temperatures differ clearly in the winter. In winter the soil temperature is much lower than on the other side and reacts to changes in the storage temperature much faster. On this side, it is almost equal to the soil temperature 1/4, which measures the temperature directly on the outside of the storage. The entire soil between the two reservoirs is, therefore, significantly colder than the soil on the other sides that is only influenced by one storage.

The other three soil sensors (1/2, 1/3, 1/4) show a similar characteristic. All of them are placed directly on the outside of the storage. As expected the temperatures are much more influenced by the ice storage. However, the temperature 1/4 on the side facing the other store is only slightly colder than that one on the other side (in comparison to the temperature 1/2). The comparison with the temperature 1/2 is regarded as more meaningful, since this one is measured by the same type of sensor. Therefore, despite the different soil temperatures at a greater distance from the reservoir, the temperature measured on the outside of the reservoir can be regarded as approximately constant around the circumference.

## 2.3 Energy balance

This sub-chapter is intended to show the energy quantities as well as the energy flows of the system. As already mentioned, the data have only been suitable for a meaningful analysis since February 2016, which is why the previously measured data are not considered here.

### 2.3.1 System energy balance

Figure 2-6 shows the heat quantity of the main system's in- and outputs per month as well as per annum. The system boundaries are selected in such a way that the energy obtained from the solar collector and the electrical energy of the heat pumps are counted as input. These are shown in the left bars. The electric energy consumption of the circulation pumps is not measured which is why they must be excluded from this analysis. The losses as well as the possible gains of the ice storage are also considered here. They are discussed in more detail in chapter *2.3.3 Energy balance of the ice storage*. The heat quantity from the solar collector is separated in the heat quantity, which is directly delivered to the heat pump and the one which is used to regenerate the ice storage. The electrical energy of the heat pumps is also divided. In this case, a distinction between the two heat pumps is made to analyse each of them individually. The heat quantities which are fed to the two storages, the SH storage and the DHW storage, are considered as output. Here again, a distinction between the two heat pumps is done. These energy flows are shown in Figure 2-5. The arrow "Solar heat to HP" and the arrow from the ice storage to the heat pumps are to be understood as meaning that both heat pumps can use the solar collector and the ice storage as source. In addition, a more detailed scheme of the overall system including the sensor positions for the measurement can be found in the appendix in Figure A- 1.

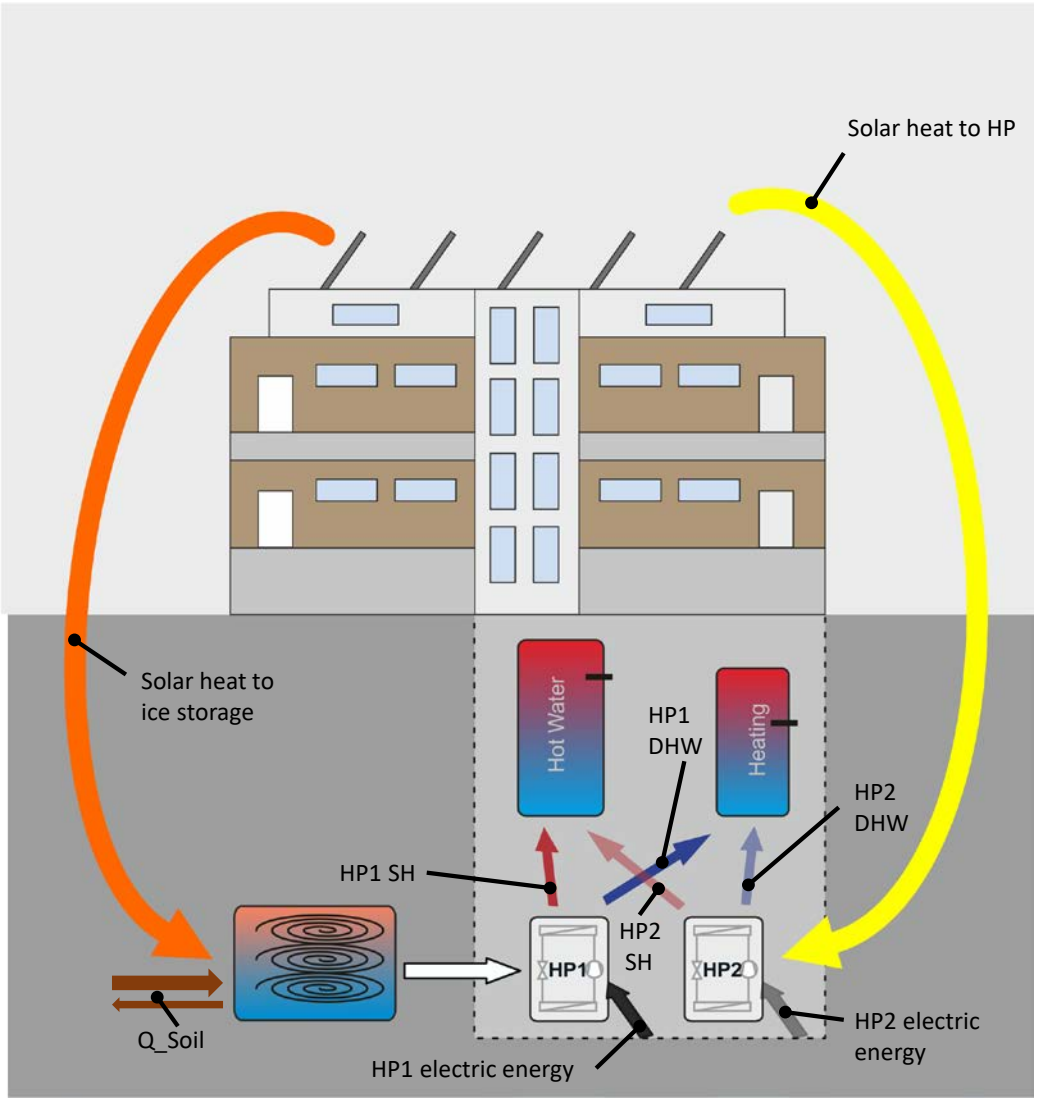


*Figure 2-5: Considered energy flows in the system energy balance*

The heat quantity of the solar collector was calculated with the measured mass flow and the measured temperature difference of the solar heat meter because of the problems described in chapter *2.1.2 The solar heat meter*. In addition, the electrical energy consumption of the heat pumps is also calculated (from the electric power) because of the in chapter *2.1.3 The electric meters* described reasons. The heat quantities supplied to the storages are known from the heat meters of the heat pumps. That means, that in case of problems with the measurement data transfer, the data from the heat meters for the heat quantities supplied to the storages is not lost, in contrast to the calculated heat quantity of the solar heat meter and the electric power consumption of the heat pumps. In Figure 2-6 only the data of the solar collector ("Solar heat to HP" and "Solar heat to ice storage") and the electric power consumption (“HP1 electric energy” and “HP2 electric energy”) is missing during the periods stated in chapter *2.1.1 Data losses*.

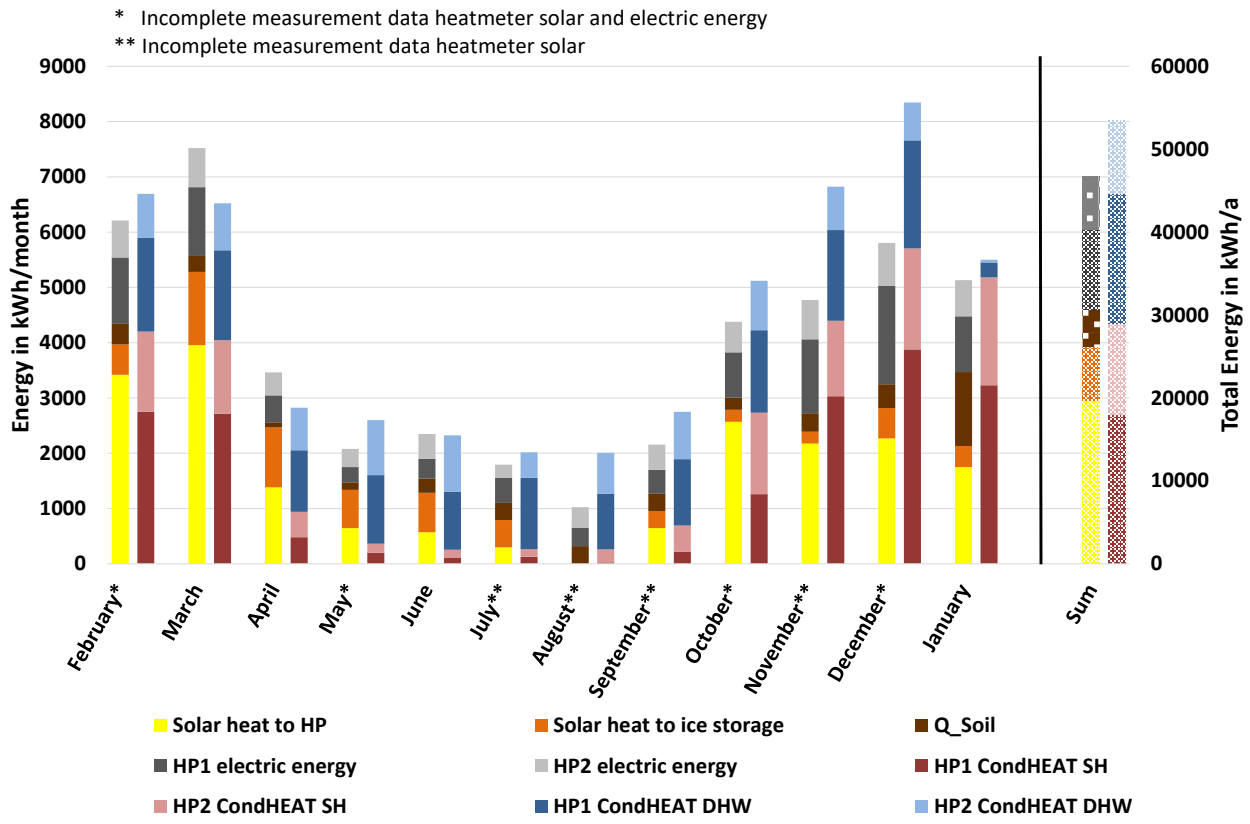


*Figure 2-6: System energy balance 01.02.2016 – 31.01.2017*

Looking at the measured values, it is noticeable that the major part of solar energy is fed directly to the heat pump during winter. This is the result of the current control, which always uses the solar collector as heat source for the heat pumps at a collector flow temperature above -4° C. The regeneration of the ice storage is further only allowed, if there is no heat requirement for the heat pumps. Since such a heat requirement occurs very often in winter, relatively little energy remains for the regeneration.

However, due to the division of the solar energy, it is not yet possible to evaluate whether there is too little energy left for the ice storage or not. If one considers the fact that the ice storage was frozen quite fast in the winter and that it took relatively long for melting again, the assumption that it would be good to get more energy in the ice storage is reasonable, because during this phase the use of the electric heating elements was necessary to cover the heat demand.

During the summer this is certainly no problem because there is more solar energy available and less energy needed. This shows a look at the right output bars in Figure 2-6 (less energy needed) as well as at the temperature of the ice storage, which in the summer reaches the maximum permissible temperature without problems (enough solar energy available to regenerate the ice storage immediately after using as source for the heat pumps). The right bars also show that the energy demand for the DHW heating is only slightly changing over the year. In the winter it is with 2500 kWh/month a bit higher than in the summer with about 2000 kWh/month.

The main difference between summer and winter is, of course, the SH requirement during the winter, which makes about 2/3 of the total heat requirement. Since even in the summer the SH storage was kept at a temperature level of 55 – 60 °C, a small amount of heat for the SH storage was needed too in these months. During this time, of course, no heat for heating was taken out of the store, which means that the energy appearing in the energy balance corresponded to the losses to the environment. This is obviously a mistake of the controller, since this approach only resulted in unnecessary losses. Therefore,

a change was requested in July 2016, so that this storage could be switched off during summer. As seen from the data from August, this change was only made for “heat pump 1”. As a result, the same heat quantity has still been used to keep the storage warm during summer, with the small difference that the energy has now been only generated by “heat pump 2”.

Furthermore, it is noticeable that in January hardly any energy was provided by the heat pumps for the DHW storage. In this month, the capacity of the heat sources for the heat pump was not sufficient. For this reason, the built-in auxiliary heater was active in the DHW storage. Because of the reason that the energy produced by the auxiliary heater is not shown in Figure 2-6, the energy supply seems to be very low in January at first view. The SH storage was still heated with the heat pumps, but for some periods the auxiliary heater was activated too for this storage. In the other considered months, the storages were never heated electrically.

The difference in Figure 2-6 between the in- and output bar of the total energy per year is mainly because of the incomplete measurement data of the solar heat meter. For the monthly consideration, the fact that the ice storage is a long-time storage which stores energy across months, is a further reason of the deviation between the two bars. In January, for example, much more energy was extracted from the ice storage than supplied. In March, the opposite was the case while the ice storage was melted.

The annual energy supply to the SH storage, referred to the heated area of 957 $m^2$, gives a specific heat demand of 30.7 kWh/($m^2$a) for the year 2016 including the losses of the storage as well as of the pipes. According to the energy performance certificate, the heat demand without losses should be 9.44 kWh/($m^2$a). Even if one considers the losses of a few kilowatt hours, the actual SH demand of the building is much higher than that calculated for the energy performance certificate! This means that the entire heating system was designed under the assumption of lower demands than actually occur.

The energy demand for DHW heating in 2016 amount to 27.4 kWh/($m^2$*a). Again, all losses of the distribution system are included, which can be considerable due to the circulation. Since the actual DHW demand is not measured, these losses cannot be quantified in detail.

In the energy performance certificate, much lower demands are expected as well. Without losses, there are only 12.78 kWh/($m^2$*a) indicated.

### 2.3.2 Energy balance of the heat pumps

After looking at the whole system, Figure 2-8 shows the heat quantities in relation to the heat pumps. In this figure, the two heat pumps are considered together. The left bars show the energy which is delivered to the heat pumps. It is distinguished whether the solar collector or the ice storage was used as source. In addition, there is the electrical energy which was supplied to the compressors. The right bars show the energy output of the heat pumps. As in Figure 2-6, this is the amount of heat which is supplied to heat the DHW and the SH storage. However, in this figure, the distinction between the two heat pumps is dispensed with. For a better understanding, this energy flows are visualized in Figure 2-7. Since this energy flows are the same for both heat pumps, only one heat pump is shown exemplary in Figure 2-7.

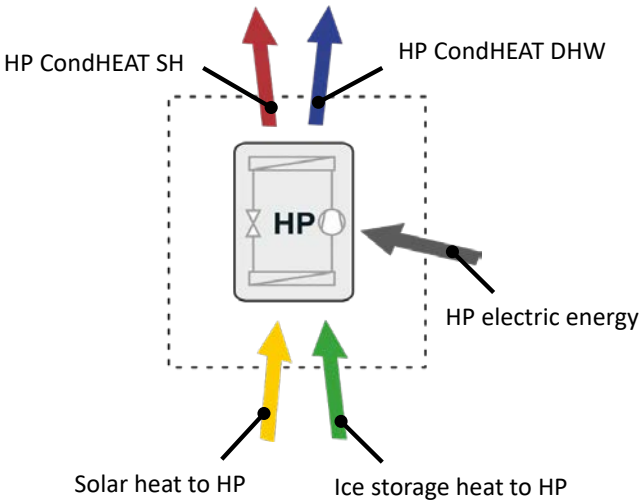


*Figure 2-7: Considered energy flows in the energy balance of the heat pumps*

The heat quantity of the ice storage as source cannot be measured directly because there is no heat meter installed at this location. Therefore, the detour via the source side of the heat pump had to be taken. With the sensor of the valve position of the heat source for the heat pumps, it is possible to distinguish whether the ice store or the solar collector function as primary source. With that, the amount of heat supplied to the evaporator can be calculated as the difference of the energy output at the heat sink side and the electrical energy. The error caused by the assumption that no losses of the heat pump occur is negligibly small.

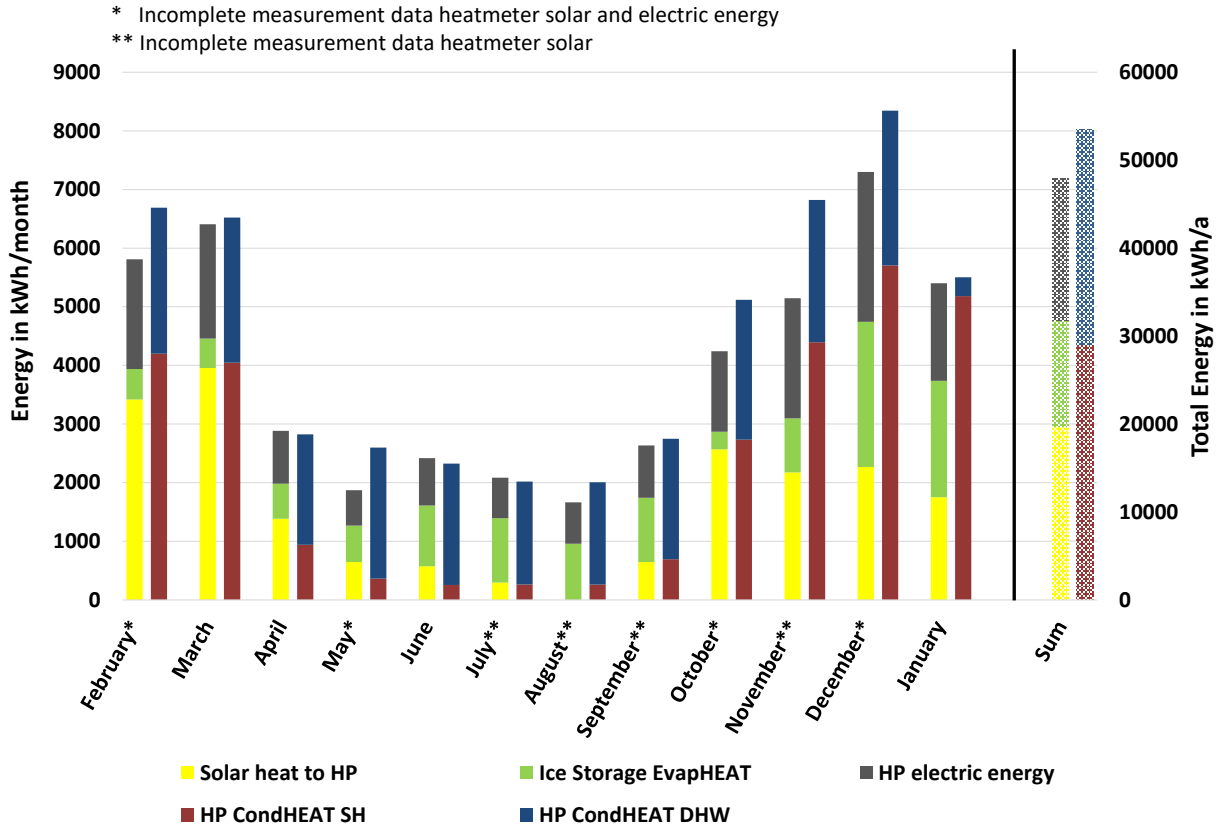


*Figure 2-8: Energy balance of the heat pumps (01.02.2016 – 31.01.2017)*

The other heat quantities shown in Figure 2-8 are calculated the same way as described in chapter *2.3.1 System energy balance*. The deviations between the input (left) and the output (right) bars are mainly because of the incomplete measurement data of the solar heat meter (Solar heat to HP) and the electric meters (HP electric energy).

If one looks at the heat quantity that is delivered to the heat pump, it is noticeable that only a small part of it is coming from the ice storage in February and March. This energy is less than 6 % of the whole delivered energy to the heat pumps, while the necessary electric energy is up to 20 %. The biggest part (~74 %) comes from the solar collector during this period. To determine the reason for this distribution, it is necessary to have a look at the ambient and the ice storage temperature too. These are shown in Figure 2-3. One can see that the ice storage temperature is around zero degree for the most time. In March, it even rises up to 5 °C. This means that the ice storage temperature is all the time in a temperature range that can be used for the heat pump. However, relatively high collector temperatures of up to 20 °C are also achieved. In addition, the collector temperature rarely drops below -4 °C and it recovers quickly during short running times of the ice storage as source for the heat pump, so that the system switches back to the collector mode soon. From the current point of view, there is nothing to say against the practice to use the collector as source for the heat pump as long as the necessary energy is available there. Nevertheless, other operation modes will be investigated for better results in the doctoral theses of Werner Lerch. (Lerch, 2017)

In the summer, the percentage of the ice storage as source rises rapidly. That is because the collector temperature is too high for the heat pump. The system works in the combined mode in which the ice storage is being regenerated and serves as a heat source at the same time (see chapter *1.4.5)*. A look at Figure 2-3 shows that this often happens in summer during the daytime. In October, it is again similar to the months of spring. The ice storage is hardly needed because the collector flow temperature is not too high, but there is still enough solar energy available to use it directly. In winter, the available solar energy decreases and the collector temperature drops more often below -4 °C. The ice storage contributes significantly to the energy supply during this phase so that the ice storage temperature drops down as well and it works as a latent storage soon. As far, this energy distribution has been quite in line with expectations. However, in the middle of December 2016, the already discussed fact occurred that the ice storages were completely frozen. As a result, in January the energy supply could no longer be covered by the heat pumps alone and the auxiliary heater had to be activated. The auxiliary heating was mainly activated in the DHW storage. Despite the fact that the auxiliary heater was not part of this energy balance, this can be seen from the heat quantity provided from the heat pumps for the DHW storage, which was quite low in January.

### 2.3.3 Energy balance of the ice storage

The energy balance of the ice storage shown in Figure 2-10 gives further insights into the functioning of the system. The energy flows, which are considered in this energy balance, are visualized in Figure 2-9 as well. The data of the amount of heat flowing from the soil into the ice storage or from the storage to the soil were calculated by using the formula (2-1).

$$Q_{Soil} = \int_{0}^{8760} U_{Store} * A_{Store} * \left(T_{Soil,m} - T_{ice}\right) * dt \qquad (2\text{-}1)$$

$A_{Store}$ is the area of the walls of the two stores, including the floor plate. The ceiling plate is neglected because there is no direct contact with the medium. $T_{ice}$ is the temperature of the ice storage and $T_{Soil,m}$ is the mean soil temperature calculated from those four sensor values which measure the temperature at the storage surface. Moreover, dt is the time step and $U_{Store}$ is the heat transmission coefficient. It has

to be noted that the amount of heat from the soil is an approximate estimate and not an exact calculation.

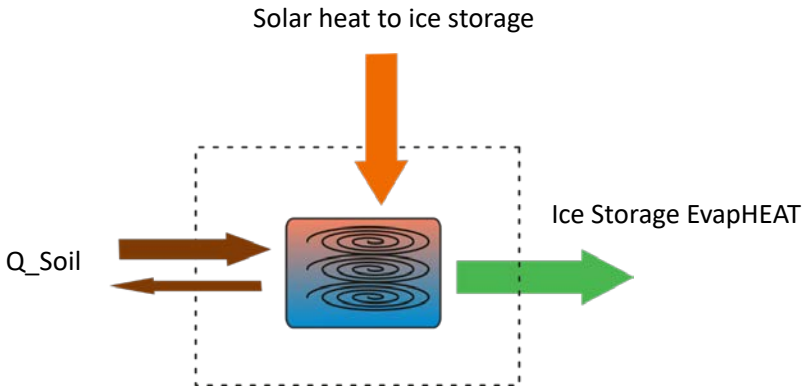


*Figure 2-9: Considered energy flows in the energy balance of the ice storage*

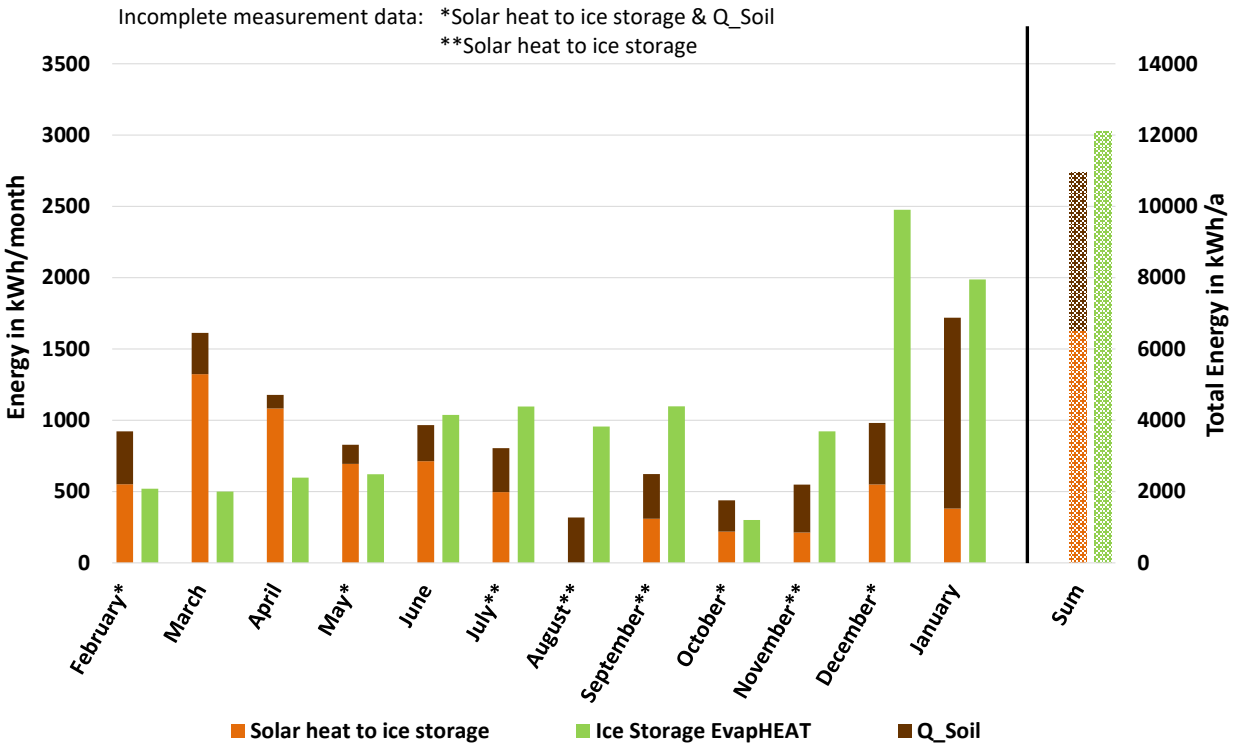


*Figure 2-10: Energy balance of the ice storage*

The data shows that for every month the amount of heat which flows from the soil into the ice storage is higher than the one which flows in the other direction. This is confirmed by Figure 2-3 which shows the ice storage temperature in comparison to the soil temperatures. The soil temperature is only a short time in April lower than the storage temperature. This means that in the rest of the time energy is extracted from the soil. Moreover, it is shown that this heat amount is a considerable part, which confirms that the burying of the ice storage in the soil pays off.

Figure 2-10 also shows that the ice storage stores the energy over a longer period. At the end of winter or in the early spring, for example, much more energy is fed into the ice storage than it emits as source for the heat pumps. During this time, the ice melts with the now again available energy. During summer, the charge and discharge energies are approximately the same because enough energy is available at the collector to reheat the ice storage to the maximum permissible temperature in a short time again

after using it as source. At the beginning of the heating season, more energy is extracted from the store. This imbalance is particularly evident in December and is the reason why the storage gets completely frozen. Due to the completely frozen storage, particularly high gains from the soil result in January, since temperature differences between ice storage and soil of up to 12 K occur in the meantime. However, the balance sheet should almost balance itself over the entire year. The reason why this is not the case, is mainly due to the data failures of the solar heat meter.

## 2.4 Performance data & auxiliary heating

In order to assess the performance of a heat pump, two characteristic numbers are used. These are the coefficient of performance (COP) and the seasonal performance factor (SPF). Moreover, the share of auxiliary heating is interesting, when evaluating the heating system.

The COP of electric heat pumps is the ratio of the useful heat output given at certain operating conditions in relation to the electrical power consumption. Therefore, the COP is measured at constant operating conditions in the laboratory and is indicated by the producer in the data sheet (Viessmann, 2015). In this case, it is 4.51 for the 6 kW and 4.72 for the 10 kW version, both for an operation point of B0W35. These values correspond to the current state of the art. However, since the system is not always operated in the standard state, the system cannot be adequately assessed alone on the base of the COP.

The SPF of the heat pumps, see eq. (2-2), is the ratio of the annual heat produced (for SH and DHW) and the amount of the used electricity (excluding the circulation pumps). It considers all operation points and other influences of the heat pump in real operation. Therefore, it is the most relevant value for assessing the actual efficiency. For the calculation, the measurement data of the year 2016 is used. This results in a SPF of 3.35 for the 10 kW and 2.96 for the 6 kW heat pump. The efficiency of both heat pumps together, according to eq. (2-3), results in a $SPF_{HP\_mean}$ of 3.20.

$$SPF_{HP,i} = \frac{Q_{cond\_HP,i}}{W_{el\_HP,i}} \qquad i = 1,2 \tag{2-2}$$

$$SPF_{HP\_mean} = \frac{Q_{cond\_HP1} + Q_{cond\_HP2}}{W_{el\_HP1} + W_{el\_HP2}} \tag{2-3}$$

In addition, the values were also determined monthly. It is shown in Figure 2-11 that the monthly SPF is lower in summer than in winter. This can be explained by the fact that in summer the heat pump is only used for the DHW heating, which requires a higher temperature level than the SH. The SH is, therefore, more economical than the DHW. However, differences can also be seen in the heating season. It is shown that the SPF is highest at the beginning of the heating period and then decreases with the ambient air temperature. This is because during the winter months the heat source temperatures are lower on the average than at the beginning of the heating period and the heat pumps work more efficiently at a lower temperature difference.

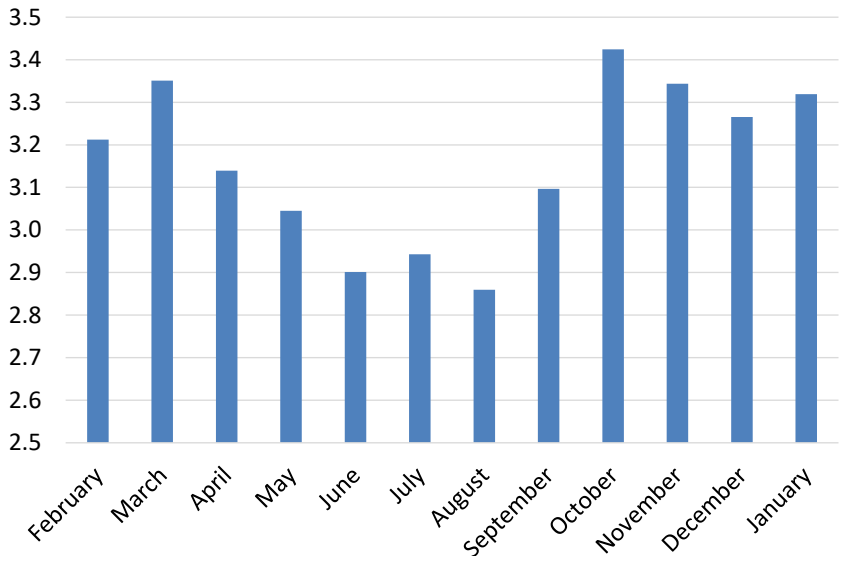


*Figure 2-11: Monthly distribution of the $SPF_{HP,mean}$ (02.2016 - 01.2017)*

Furthermore, it would be interesting to know the SPF of the overall system because it has an even greater significance than the consideration of the heat pumps alone. The SPF of the overall system would also be a good indicator for comparing this system to other heating systems as, for example ground-source heat pumps. Since, however, necessary measured values are missing, this consideration must be dispensed with at this point, but in the Austrian report on HPT Annex 50 - Task 3.2 System Performance Factors determined by means of a validated simulation model are presented.

The share of the auxiliary heating is also an interesting value of a heating system. In the considered measuring period, the auxiliary heating was activated at the end of December and in January, when the ice storage was subcooled. During this time especially the required energy for the DHW storage was provided from the auxiliary heating. With the equation (2-4), the share of the auxiliary heating results in 4.8 % corresponding to 2712 kWh/a in total numbers.

$$EHeat = \frac{Q_{aux}}{Q_{cond\_HP1} + Q_{cond\_HP2} + Q_{aux}} \quad (2\text{-}4)$$

This share of 4.8 % is quite satisfying, if one considers the subcooling of the ice storage for a period of about one month. But an evaluation of the system on the basis of this share is difficult since the share of auxiliary heating can change considerably between years. Therefore, a consideration of a longer period (some years) would be necessary for a meaningful evaluation. However, in Chapter 4 the SPF of the system has been evaluated following eq. (2-5).

$$SPF_{System} = \frac{Q_{eff\_SH} + Q_{eff\_DHW}}{Q_{el\_HPs} + Q_{el\_pumps} + Q_{aux}} \quad (2\text{-}5)$$

# 3 Optimization potentials and error prevention

This Chapter deals with the optimization potentials and error preventions which are already implemented in the system in Weiz. Moreover some possible improvements are analysed with the validated simulation model but not yet implemented in the real system. These improvements are discussed in the Austrian report on HPT Annex 50 – Task 3.2.

## 3.1 Controller problems of the second heat pump

The data analysis of the first heating season showed that the controller of heat pump 2 (HP 2) was not optimal adjusted. As shown in Figure 3-1 there were some periods in which the temperature of the DHW storage dropped below 40 °C. Despite this high heat demands only the heat pump 1 (HP 1) was working, while HP 2 was deactivated. It turned out, that because of a wrong setting HP 2 was always turned off when the evaporator temperature (brine flow temperature) dropped below -4 °C.

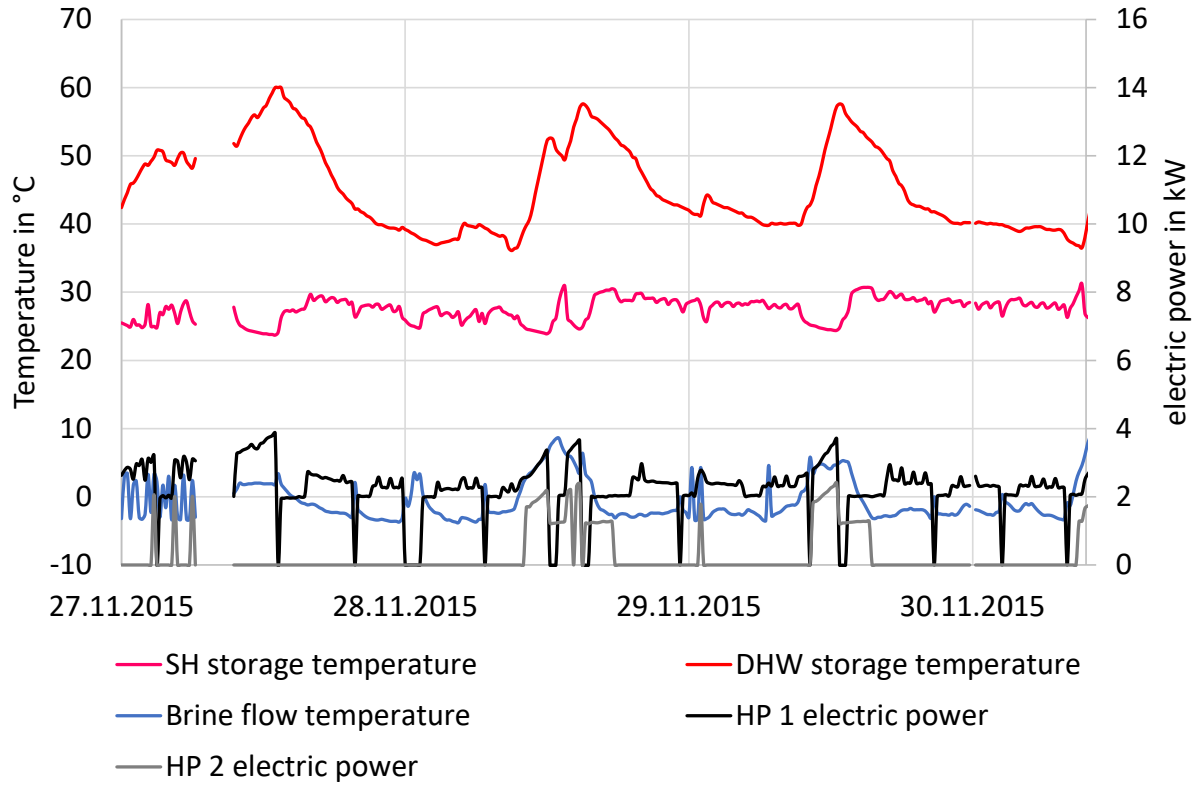


*Figure 3-1: Wrong setting heat pump 2*

The left part of Figure 3-2 shows this problem again. Despite the fact that the required heat demand was too big to get provided with only one heat pump, HP 2 has not been activated. As a result, the auxiliary heating has to be activated to hold the temperature level of the DHW storage in the desired area. The wrong setting was corrected on the 17.12.2015. It can be seen in Figure 3-2 that since this time the heat pump 2 is used more often and that the both heat pumps together provide enough energy so that the auxiliary heating was not necessary any more.

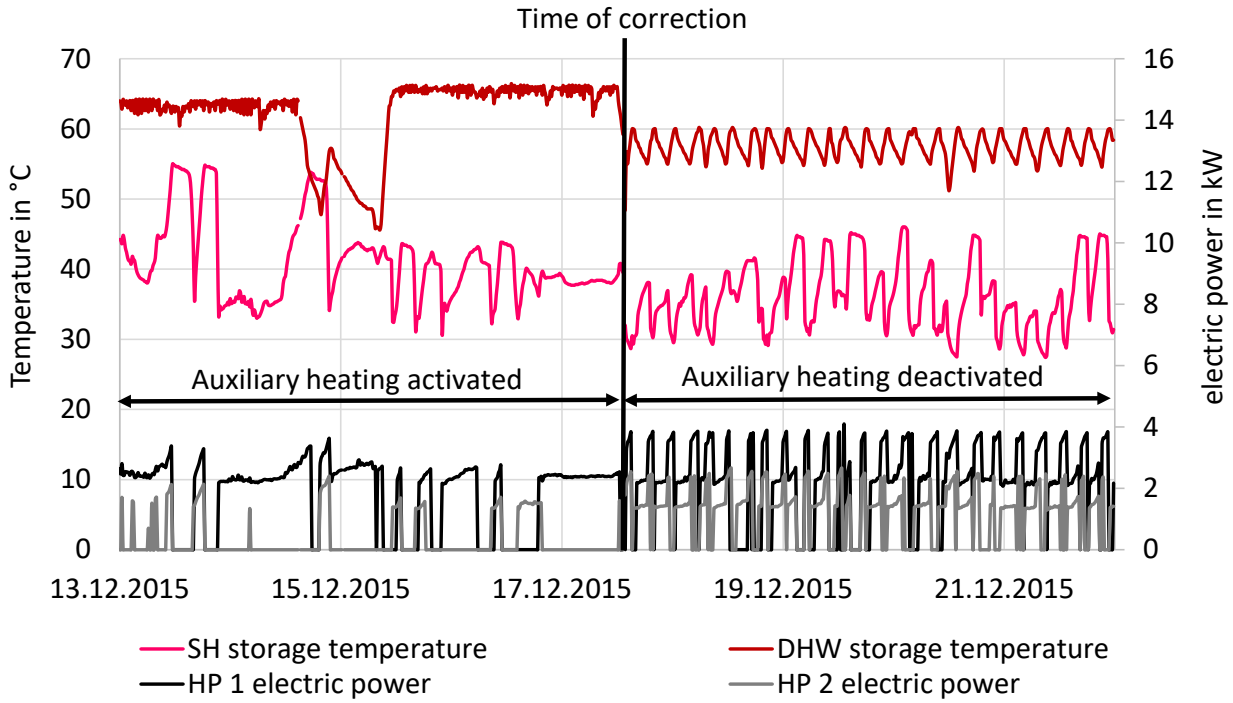


*Figure 3-2: Correction of the wrong setting*

## 3.2 Heating of the SH storage during summer months

As shown in Figure 2-6 the heat meters of the SH storage count a heat quantity of some kWh also during summer. A look at the temperature of the SH storage in the summer months, shown in Figure 3-3, show, that the storage has temperatures up to 60 °C. A controller failure was expected, so that a modification of this setting was requested.

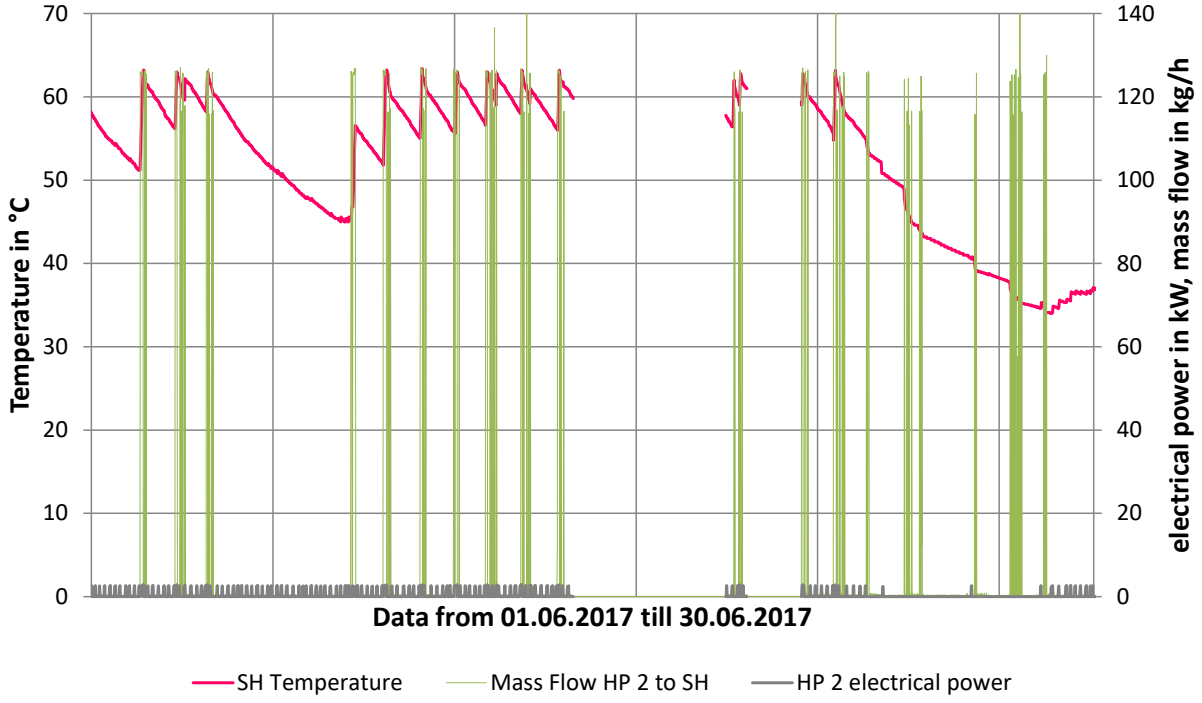


*Figure 3-3: SH temperature trend in June 2017*

## 3.3 Optimization of the maximum ice storage temperature during summer months

Another problem occurred during the summer months concerning the ice storage temperatures. Most times during the summer the system works in the combined mode (see section *1.4.5), i.e.* the ice storage is used as source for the heat pumps and is regenerated at the same time. The maximum set temperature for the regeneration is 15 °C. Therefore, this is the temperature the ice storage has the most time during summer. If the ice storage is used for cooling its temperature can be even higher because the return temperature from the floor cooling is higher than 15 °C and heats the storage additionally. The problem was, that the heat pumps are deactivated automatically when the source temperature on the evaporator side exceeds 20 °C. Therefore, it happened, that neither the ice storage nor the solar collector could be used as source for the heat pumps because they both were too hot. This in turn means, that the auxiliary heating had to be activated in the DHW storage. If the ice storage is still used for cooling the problem becomes worse, because the ice storage is heated more and more from the return flow of the floor cooling, but is not cooled anymore as it would be the case, if it would be used as source for the heat pumps.

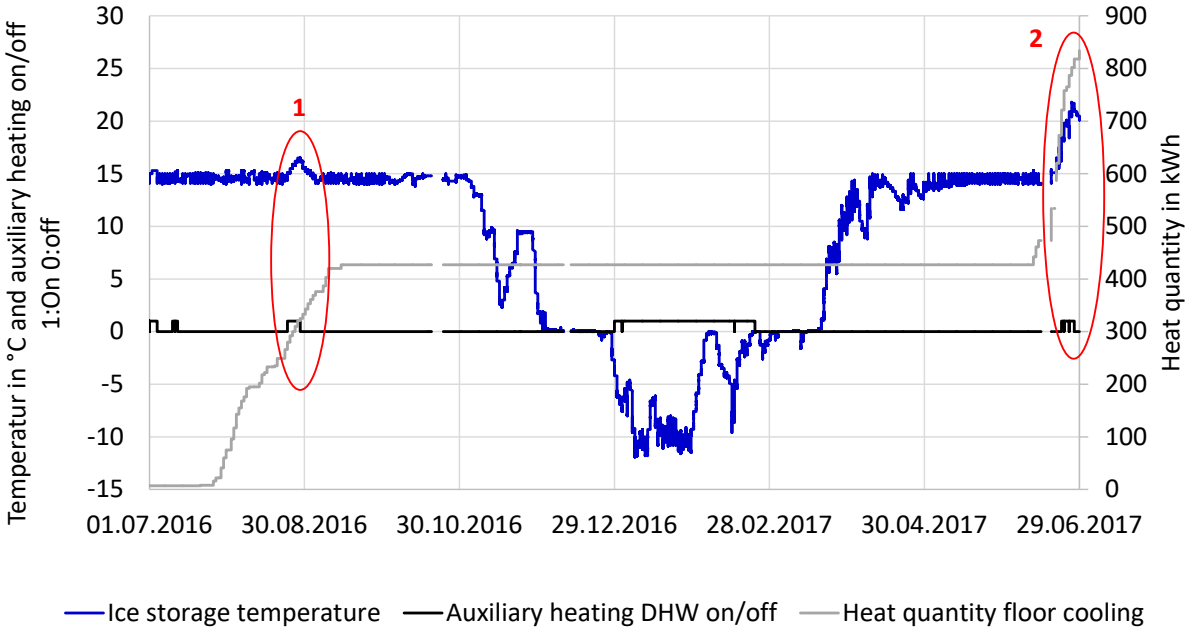


*Figure 3-4: Ice storage problem areas overall view*

As shown in Figure 3-4, this problem occurred in summer 2017 as well as in summer 2016. While in 2016 only a short increase of the ice storage temperature of about 2 K occurred, in 2017 the temperature rose up to more than 20 °C for a longer time. This results in an unnecessary use of the auxiliary heating. Both areas are displayed in more detail in Figure 3-5 and Figure 3-6.

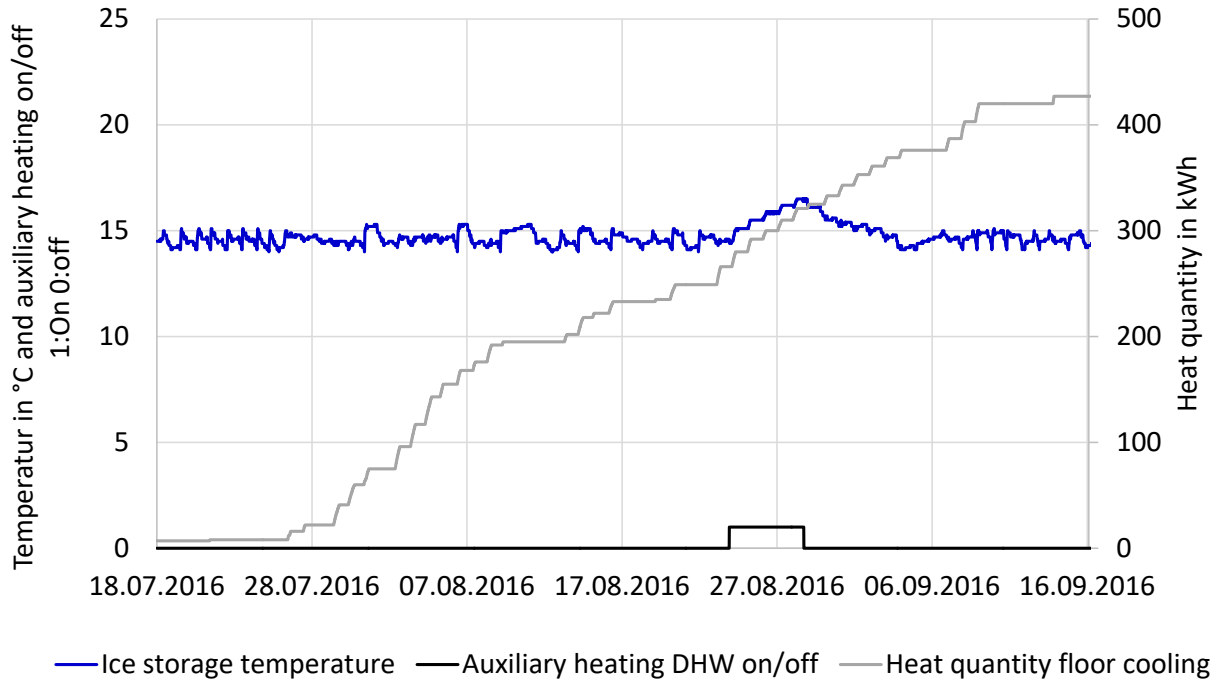


*Figure 3-5: Ice storage - Problem area 1*

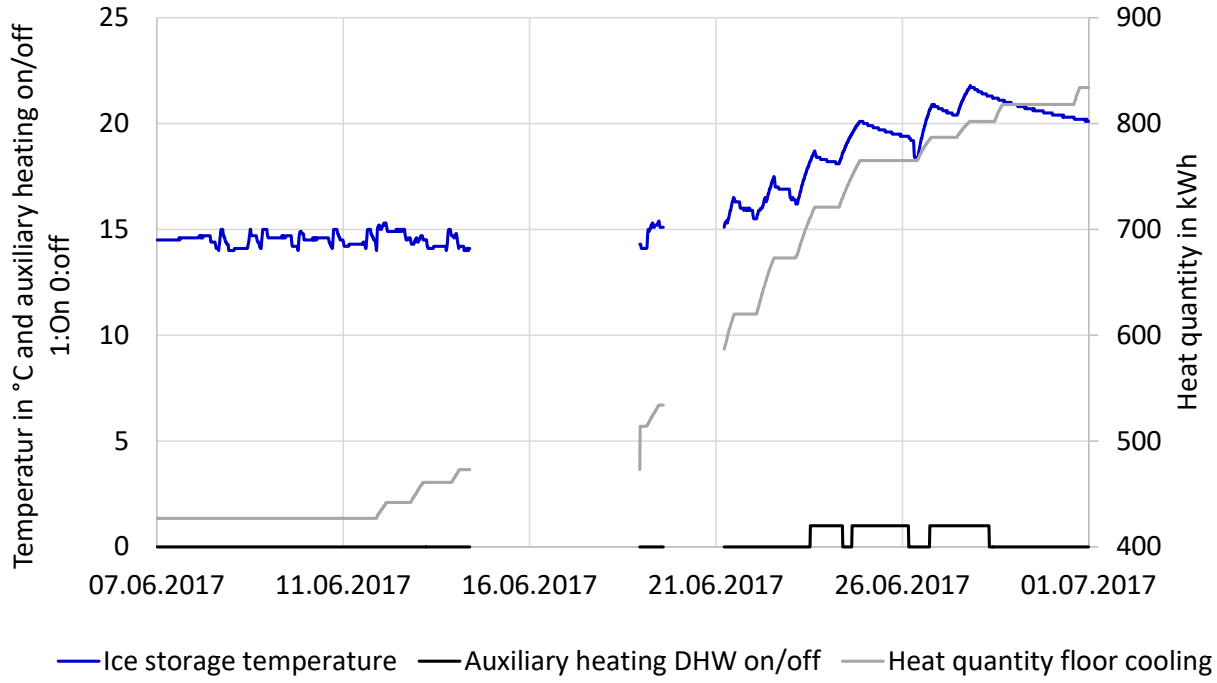


*Figure 3-6: Ice storage - Problem area 2*

In order to solve the problem discussed above, an improvement was attempted in summer 2020 by modifying the heat pump control. On the one hand, the maximum temperature of the ice storage tank was increased from 15 to 25 °C. On the other hand, an improvement of the active regeneration of the ice storage tank in summer by the solar collectors from a maximum temperature of 15 °C to 12 °C was attempted. This should provide a lower temperature level for cooling via the floor heating system. Unfortunately, these planned controller settings could not be implemented by the operator so far, but will be done by a technician in the course of the next service.

# 4 Measurement Results for the Period January 2017 to April 2020

For the general proof of the operation and efficiency of the real plant, the measurement data for the period from the end of 2017 to the beginning of 2020 were analysed and evaluated. Due to some measurement data failures, the analyses carried out are sometimes incomplete. With regard to the optimisation measures identified, such as an enlargement of the ice storage tank, an enlargement of the collector surface (see Austrian Task 3.2 report), a preliminary monetary evaluation was carried out and discussed with the operator. Due to the associated conversion costs, no further improvements could be implemented except for the changes in the control system, which have already been proposed and presented on the base of the measurement results discussed in Chapter 2 and 3.

Data losses

During the analyzed measurement period from 01.01.2017 until 10.04.2020, some longer data failures have occurred. For the following periods no measurement data is available:

- 26.9.2018 - 7.11.2018
- 23.11.2018 - 3.12.2018
- 25.12.2018 - 21.1.2019
- 9.2.2019 - 18.2.2019

The data losses of the whole system were caused by data transfer problems. That means that the sensors worked correctly during these times, which is particularly important for the heat quantity data recorded by the heat meters. Thus, the heat quantities are available without losses for the (monthly) energy balances.

Additionally, it happened sometimes that single measured values (e.g. capacities and temperatures) are missing. These short data losses, however, are in a range that no substantial influence on the further data evaluation can be assumed.

Source and sink temperatures of heat pumps

In order to be able to evaluate the efficiency of the solar ice storage heat pump system, it is essential to know the boundary conditions under which the heat pumps are working. Figure 4-1 shows the load duration lines of the temperature sensor in the upper part of the hot water storage tank, the heating storage tank and the flow and return temperatures of heat pump 1 (see Figure 1-2 - Scheme). The flow and return temperatures of the heat pump are shown separately for the case of hot water preparation and space heating. In order to increase the efficiency of the overall system, the operator has reduced the set point temperature for domestic hot water preparation by approx. 5 K to about 55 °C (the remaining heat demand is provided by an E-cartridge). Thus, the return line of the domestic hot water circulation loop has a temperature of around 50 °C and the mixing with the hot water in the storage reduces the temperature leading to rather long running times of the heat pump and a high energy demand. On the space heating side, significantly lower temperatures are required with a similar heat pump running time.

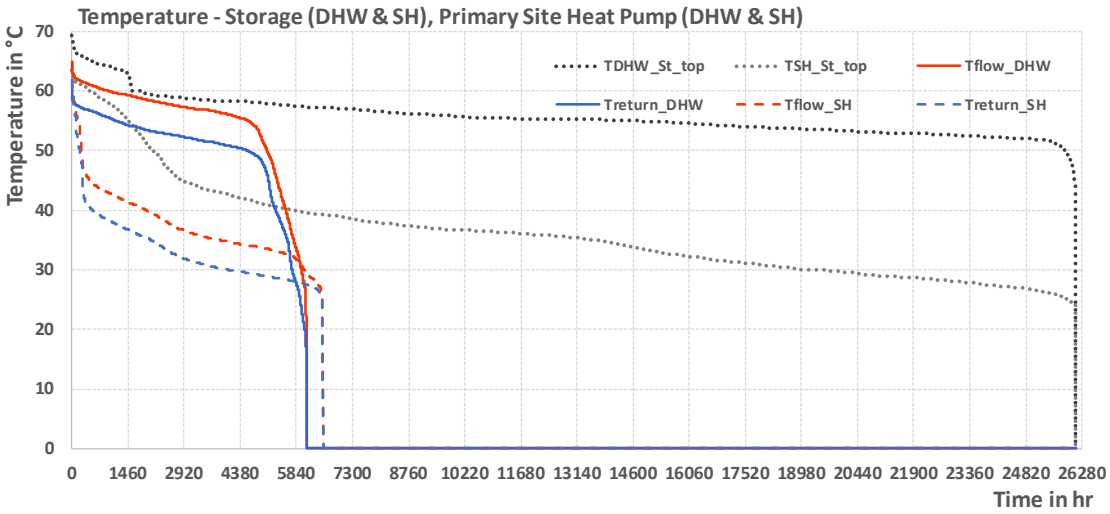


*Figure 4-1: Duration curves of Temperatures – DHW-storage at the top, and flow and return temperature (SH & DHW-Mode) (Heat Pump 1, 01.2017 - 04.2020)*

In order to achieve an efficient operation of the heat pump, a high evaporator temperature (= source temperature) is advantageous in addition to a low condenser temperature (= sink temperature). Figure 4-2 shows for heat pump 1, in addition to the primary flow and return temperature, the secondary flow and return temperature on the source side. It can be seen here that during almost half of the operating time, the source temperatures are higher than 0°C. The minimum occurring temperatures are in the range of about -10 °C.

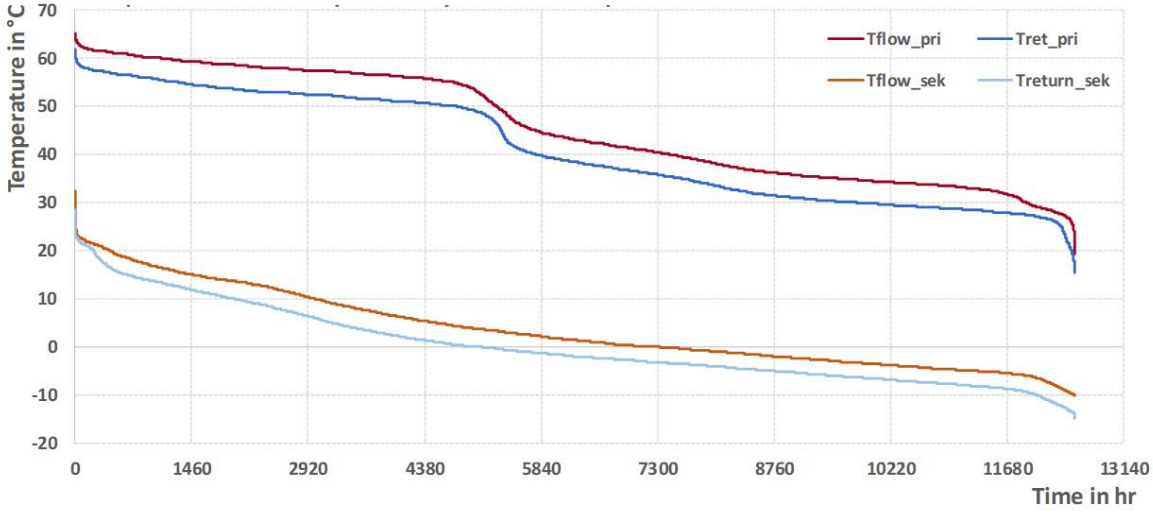


*Figure 4-2: Duration curves of flow and return temperatures on the heat sink ("pri") and heat source side ("sek") (Heat Pump 1, 01.2017 - 04.2020)*

Power curves of the heat pumps in domestic hot water and space heating operation

The nominal outputs (B0/W35) of the two heat pumps are around 10 kW (HP1) and 6 kW (HP2). Depending on the boundary conditions with regard to the source and sink temperatures shown above, the two heat pumps have significantly higher or lower outputs and performance factors. Figure 4-3 and Figure 4-4 show the load duration curves of the outputs of the two heat pumps and the solar thermal system. The Figure 4-3 shows the performance curves, separated according to the applications domestic hot water preparation and space heating. On the one hand, it can be seen that the output of the solar

thermal system with a maximum of 12 - 14 kW corresponds approximately to the larger of the two heat pumps. A comparison of the applications shows that the heating storage is charged at a significantly higher power than is the case for domestic hot water preparation. This is due to the higher sink temperatures during domestic hot water preparation outlined above.

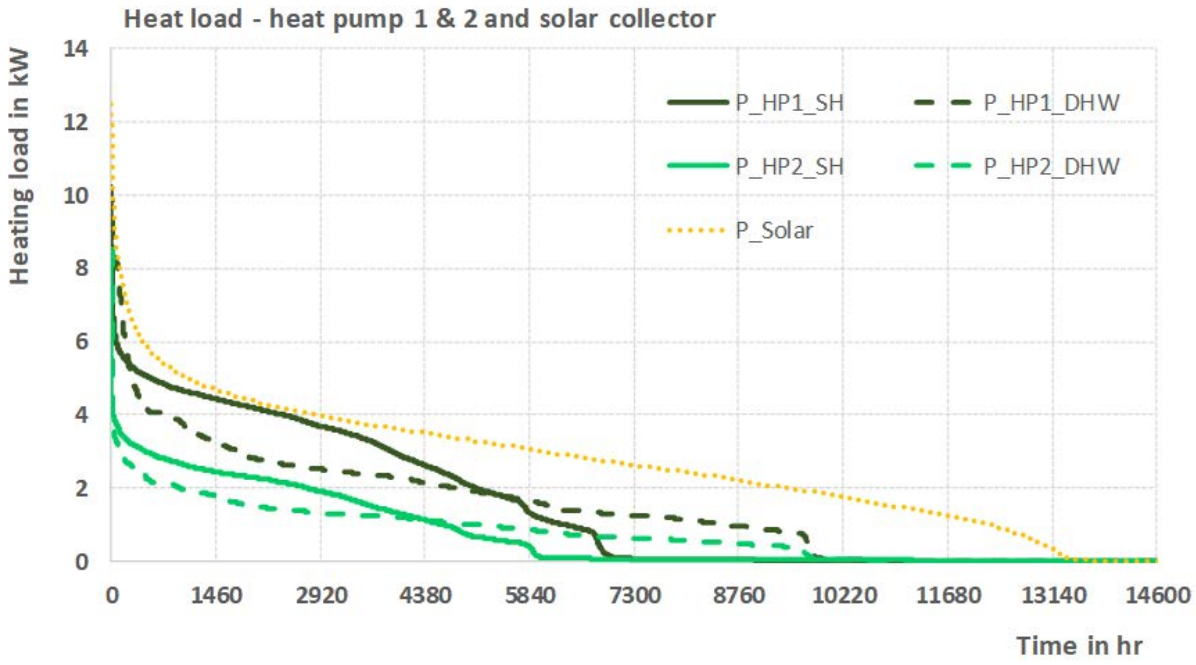


*Figure 4-3: Duration curves for the load of the heat pump 1 & 2 and the solar thermal system, separated according to the use of the heat (DHW & SH) (01.2017-04.2020)*

If one looks at Figure 4-4, in which the output curves are only differentiated for heat pumps but not for applications, a similar characteristic of the two differently sized heat pumps can be observed power classes. What is also evident is that the solar system appears to be somewhat undersized in terms of its size, as the possible output is only approximately that of heat pump 1 with 10 kW (B0/W35). In fact, in addition to regenerating the ice storage tank, the solar thermal system should also be used as a direct air/brine heat exchanger, although in this case the output appears to be too low.

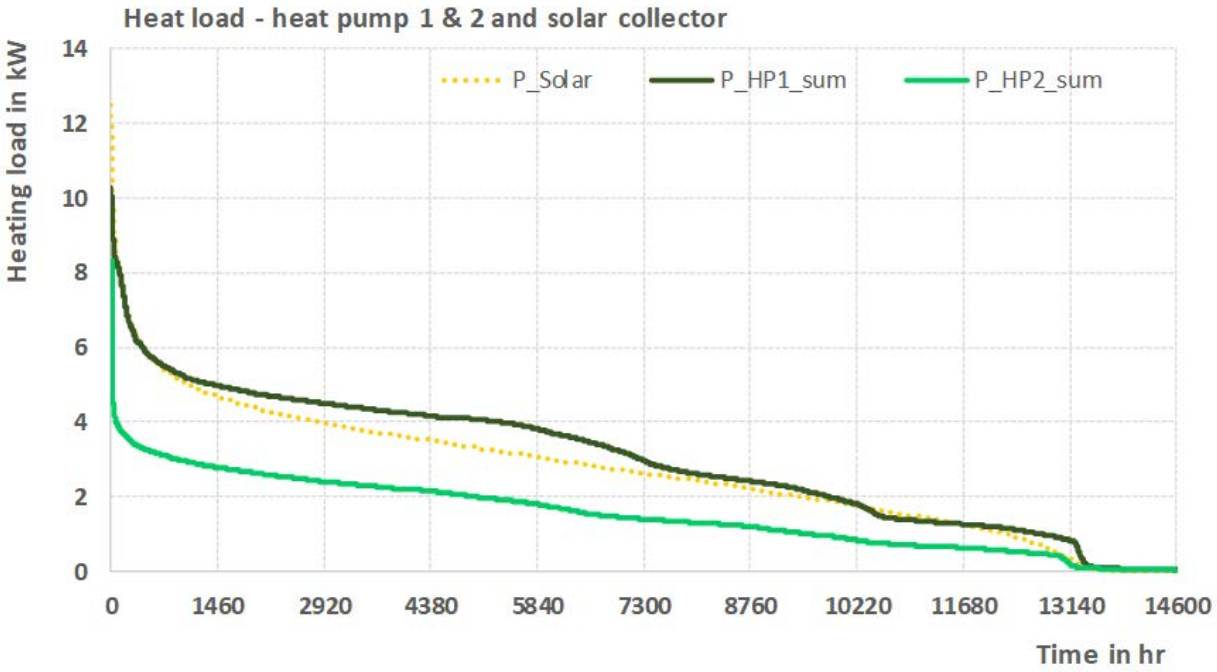


*Figure 4-4: Duration curves for the load of the heat pump 1 & 2 and the solar thermal system (01.2017-04.2020)*

Heat source of the heat pump: ice storage, ground and solar thermal collector temperatures

In addition to the heat source solar thermal energy, the ground and ice-storage temperatures will also be considered. Figure 4-5 shows the trend of all available ground temperatures, which are located in the periphery of the two uninsulated ice storage tanks (see Figure 1-6). With regard to the ground temperatures, it can be seen that the minimum temperatures are close to 0 °C, although at this point in time the temperature sensors further away still have around 5 °C. In the summer months, maximum temperatures between 20 and 24 °C are reached. Over the three years, a slight increase in minimum temperatures can be seen with regard to the minimum ground temperatures in the winter months.

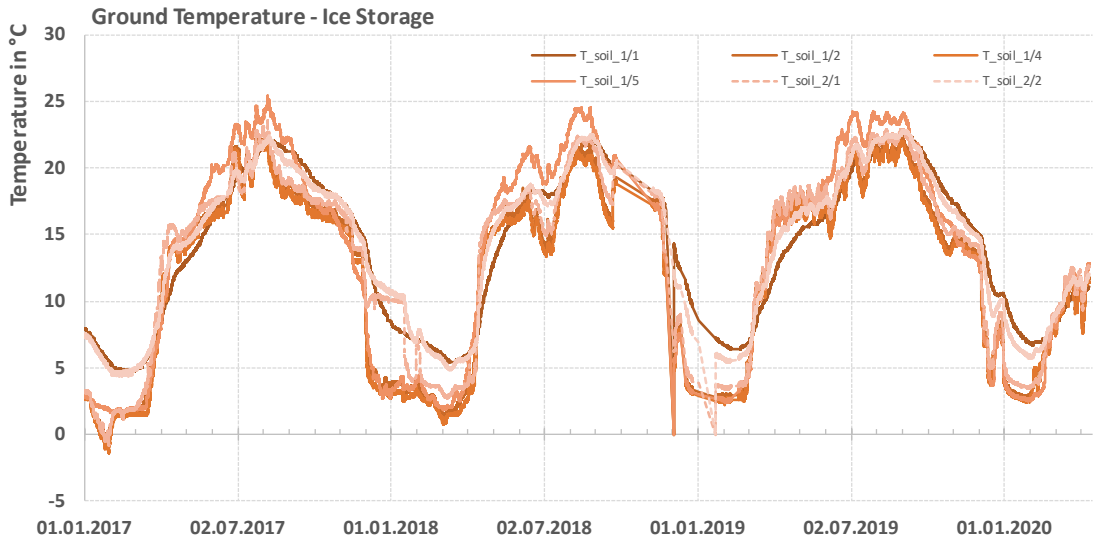


*Figure 4-5: Ground temperatures around the two ice storages in different positions (see Figure 1-6)*

In addition to the ground temperatures, the temperatures in the ice storage are essential when it is used a direct heat source. These temperatures as well as the times with activated E-cartridges are plotted in Figure 4-6. Every autumn a similar picture appears. The ice storage tank, charged to approx. 20-25 °C, is discharged to about 0 to 5 °C within a few weeks. At this temperature level, the ice storage units are usually operated until the beginning of January and then the storage fluid is completely frozen and becomes sub-cooled, thus the temperature drops to ca. -10 °C within a few days. At this time the E-cartridge is started up manually. This phase usually takes between two weeks and one month until the temperature level in the ice storage unit recovers. Furthermore, it can be seen that the climatic conditions in winter 2019/2020 have changed significantly towards higher outside air temperatures. In this winter, the ice storage is in phase change for about two months, but the storage does not freeze through completely this year. This has been achieved by the fact that the E-cartridges were activated at the end of January, shortly before the storage tank was completely frozen.

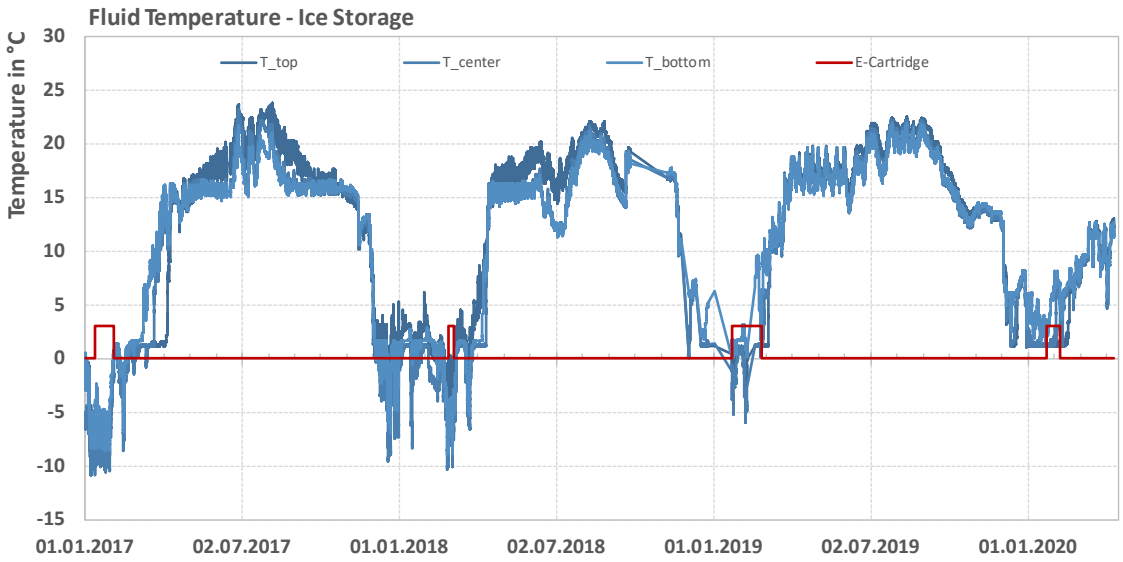


*Figure 4-6: Ice storage fluid temperatures in different layers and on/off times for the E-cartridges (SH & DHW storage)*

The following diagram (Figure 4-7) shows the interaction of the heat sources (solar thermal, outside air) and the ice storage as well as the associated ground. The ground temperatures and ice storage temperatures are shown as averaged temperatures for the first ice storage tank. The outside air as a heat source (indirectly via the solar collector) is highly fluctuating and quickly reaches temperatures that are too high for direct use with the heat pump. This also applies to direct use of the heat from the thermal solar collector. The not directly usable heat is stored in the ice storage tank, as long as it is not too warm. The temperature level of the ice storage tank provides the most uniform source temperature for the heat pump, whereby the insufficient dimensioning causes problems with the complete freezing of the ice storage tank. This leads to an increased electricity demand due to the necessary use of the E-cartridges.

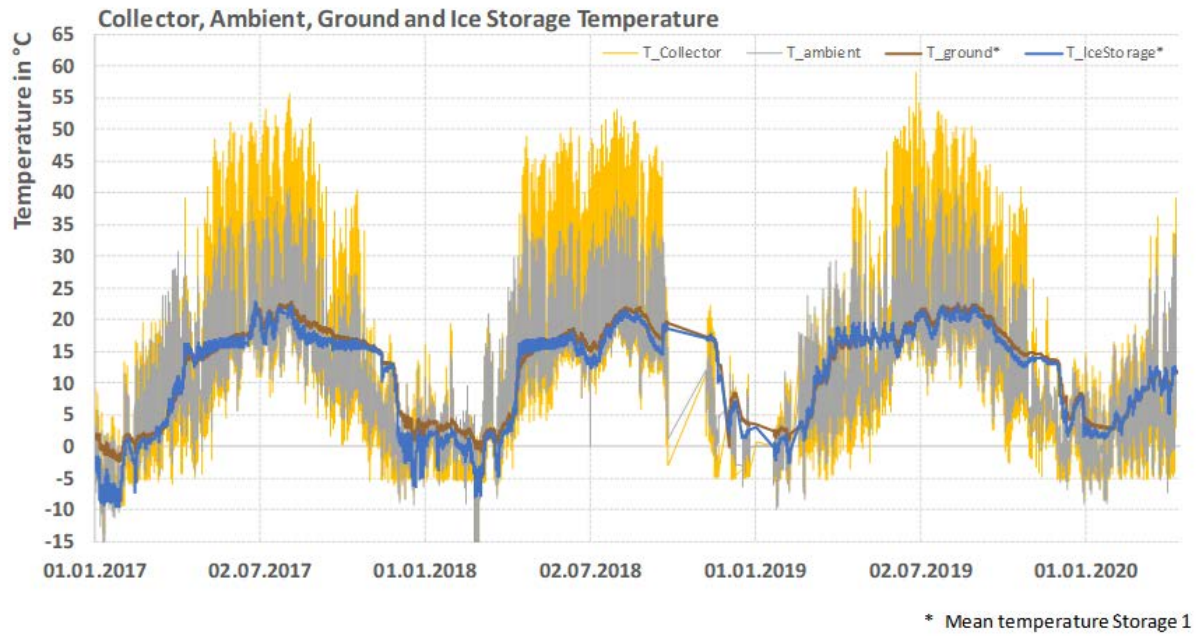


*Figure 4-7: Ambient temperature, collector temperature, mean ice storage fluid temperature and mean ground temperature (only for the first ice storage tank)*

Energy balance of the solar ice storage heat pump system for the years 2017, 2018 and 2019

At this point an attempt was made to draw up an energy balance for the two heat pumps (HP). Due to missing measurement data (detailed times see above; power and temperatures are missing), it was not possible to determine all energy balances on a monthly basis. However, the missing data was estimated based on the other years of measurements to be able to show a complete picture. Thus, monthly resolved energy balances of the system can be shown. The energy balance shows the monthly values (left axis) and the annual values on the right axis. Three bars are shown for each period (monthly and annual values).

The first bar shows the thermal source or electricity demand of the heat pumps. On the one hand, the heat drawn directly from the solar thermal system (Q_solar_to_HP), the heat extracted from the ice storage tank by the heat pumps (Q_ice_to_HP) and the electricity required for the heat pumps (P_el_HP) are shown. The second bar shows for each heat pump those parts of the energy for space heating and domestic hot water preparation. Thus, the heat supplied to the energy storage tank for space heating (Q_HP_SH) and the heat supplied to the energy storage tank for domestic hot water (Q_HP_DHW) can be found broken down by heat pump. In addition, the electricity required for the electric heating cartridges (Q_EC_sum) is also shown here. The third bar summarizes the heat supplied by the heat pumps and the electrical cartridges to the two storage tanks in terms of use (space heating (Q_DHW) and hot water (Q_SH)).

Figure 4-8 to Figure 4-10 show the energy balances for the last three years 2017, 2018 and 2019, although in some months the balances were not fully available and were therefore estimated using the ratios of the corresponding months of the other years. The HP1 with about 10 kW (peak load @ B0/W35) always delivers more energy over the three years than the second, smaller HP2 (6 kW - peak load @ B0/W35). In total over the three years, HP1 in average ca. 35 MWh/a. The HP2, on the other hand, delivers in average ca. 18 MWh/a.

In total, over the three years, the share of the energy supplied to the two storage tanks amounts 52 % and 48 % for space heating and domestic hot water, respectively. Specifically, this means a heat input to the heating storage of 23 kWh/(m²a) and to the domestic hot water tank of 21 kWh/(m²a). These values

are significantly higher than the forecast values according to the official buildings Energy Performance Certificate which indicates useful energy demands of 9.5 kWh/(m²a) and 14.6 kWh/(m²a), respectively.

Regarding the distribution between space heating and hot water preparation, HP1 shows a ratio of 53 to 47 %. HP2 shows a ratio of 51 to 49 %. Space heating is dominant in the winter months. In the summer months, domestic hot water preparation is the dominant mode of operation. These basic relationships can be seen in all three years. Each year, a total of about 51 – 53 MWh was delivered to the system by the two heat pumps.

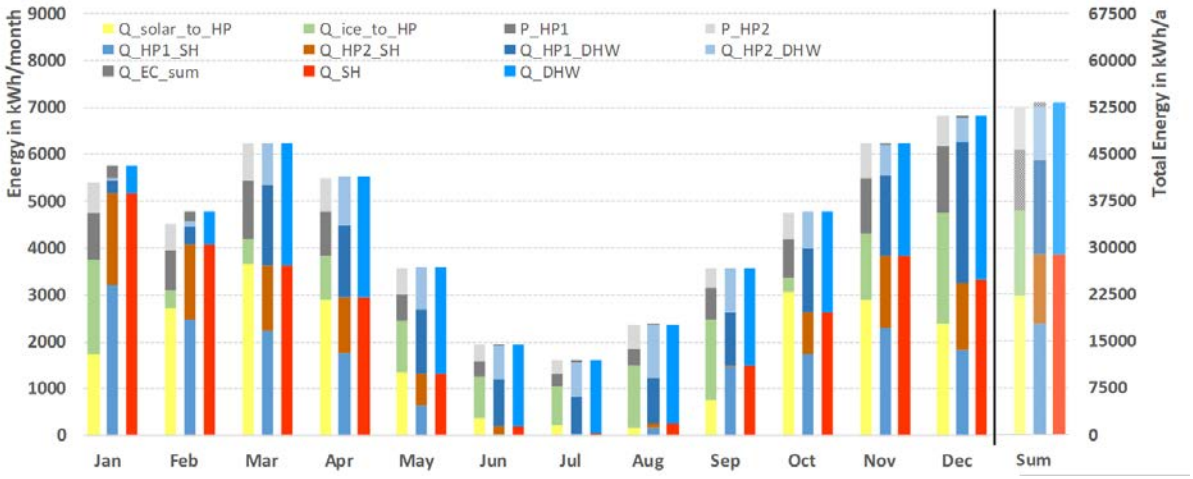


*Figure 4-8: Energy balance - heat pumps (01.01.2017 – 31.12.2017)*

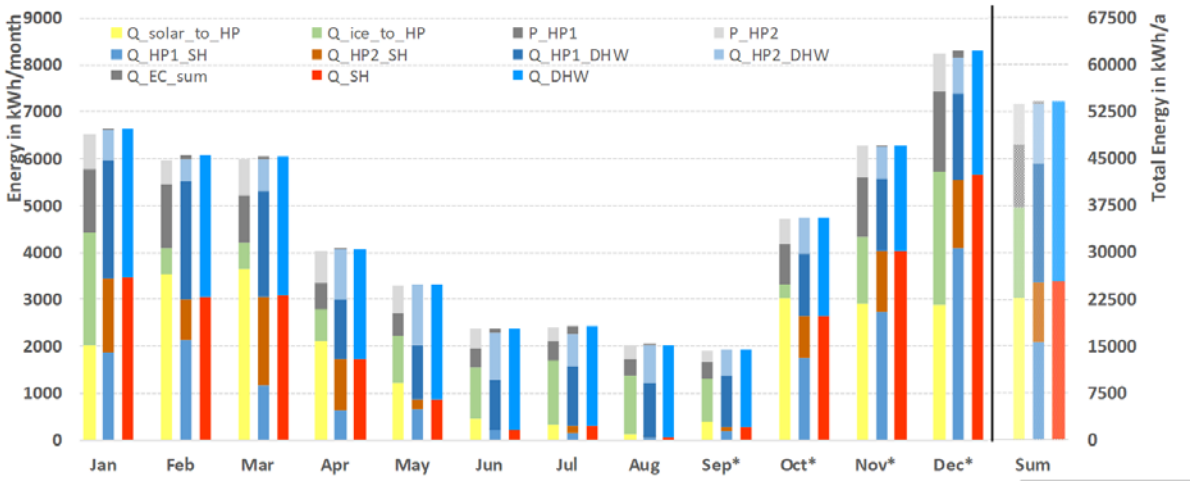


*Figure 4-9: Energy balance - heat pumps (01.01.2018 – 31.12.2018) (*partly missing measurement data)*

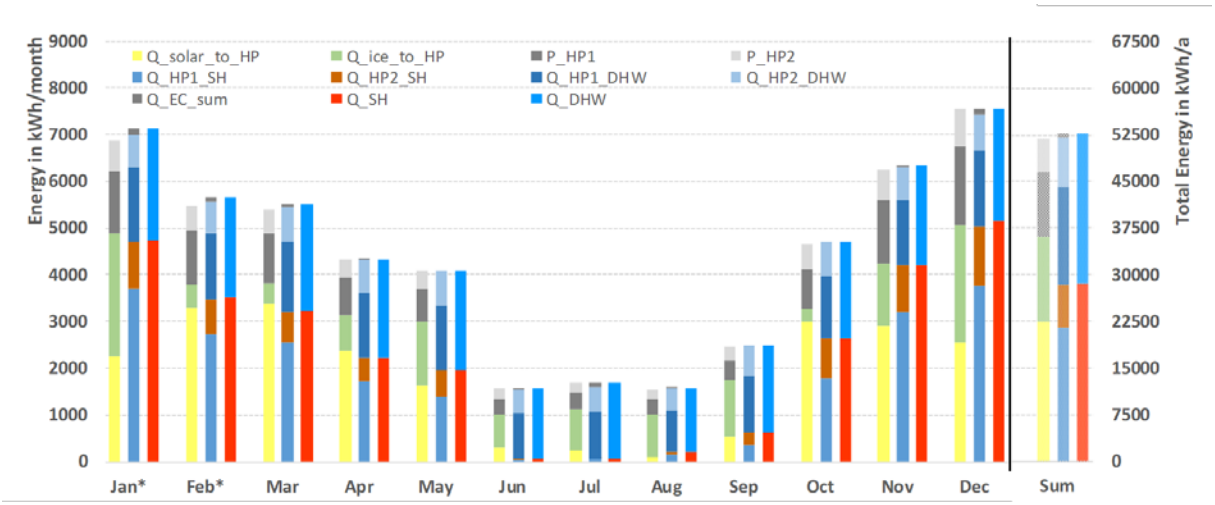


*Figure 4-10: Energy balance - heat pumps (01.01.2019 – 31.12.2019) (*partly missing measurement data)*

Table 4-1 shows the comparison of the SPFs of the individual years, the different HPs and the mean values of the HP-SPFs and the system SPFs.

Over the years, there are only minor differences in the SPFs determined acc. to Eq. (2-1) (approx. ± 2 %). The differences between the two HPs are significantly larger. In the reference case (B0/W35) the difference is only about 5 %. In real operation, however, the difference is on average 22 %. This means that the smaller heat pump (HP2) cannot handle efficiently the given conditions such as high flow temperatures and a slightly higher share of domestic hot water. In total, the two HPs have a common $SPF_{sum}$ (= $SPF_{HP\_mean}$ acc. to Eq. (2-3)) of 3.2 to 3.3. Taking into account the E-cartridges within the two energy storage tanks, the $SPF_{SumSys}$ (= $SPF_{System}$ acc. to Eq. (2-5)) is ca. 3.1.

*Table 4-1: Seasonal performance factors as well as the reference COPs of the heat pumps (at B0/W35)*

| | **SPF HP1 (10 kW)** | **SPF HP2 (6 KW)** | **$SPF_{sum}$** | **$SPF_{SumSys}$** |
|---|---|---|---|---|
| **2017** | 3.42 | 2.89 | 3.20 | 3.08 |
| **2018** | 3.43 | 2.91 | 3.22 | 3.12 |
| **2019** | 3.57 | 2.77 | 3.30 | 3.19 |
| **B0/W35** | 4.72 | 4.51 | | |

Figure 4-11 to Figure 4-13 show the monthly values of the SPFs of the two heat pumps and the whole system ($SPF_{SumSys}$) for the last three years 2017, 2018 and 2019, although in some months the balances were not fully available and were approximated using the appropriate months of the other years.

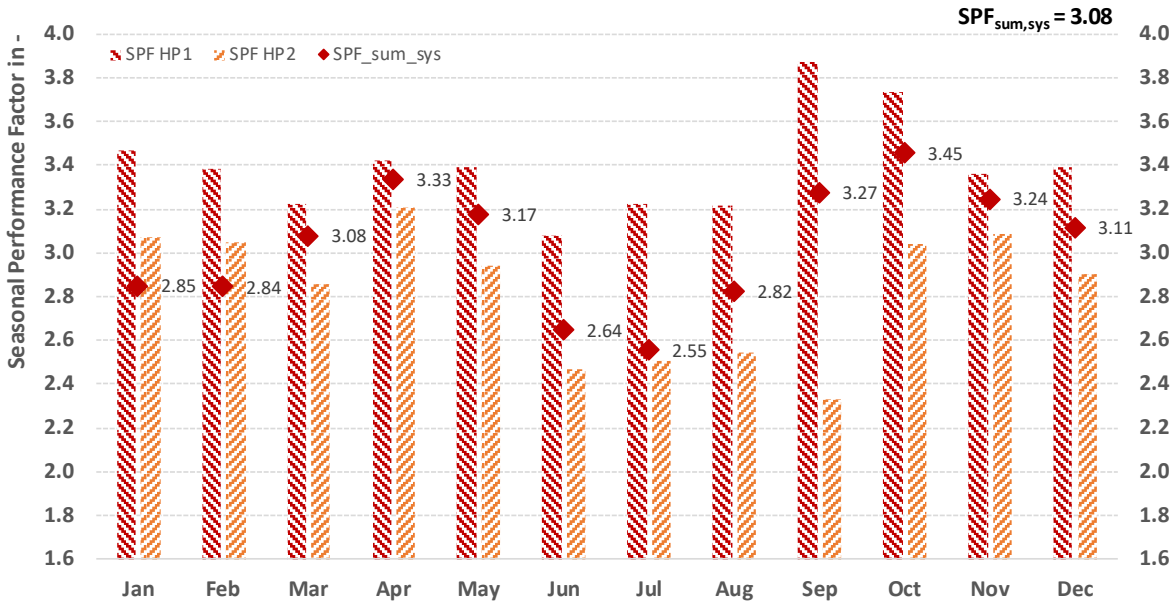


*Figure 4-11: SPF of the two heat pumps and the system (01.01.2017 – 31.12.2017)*

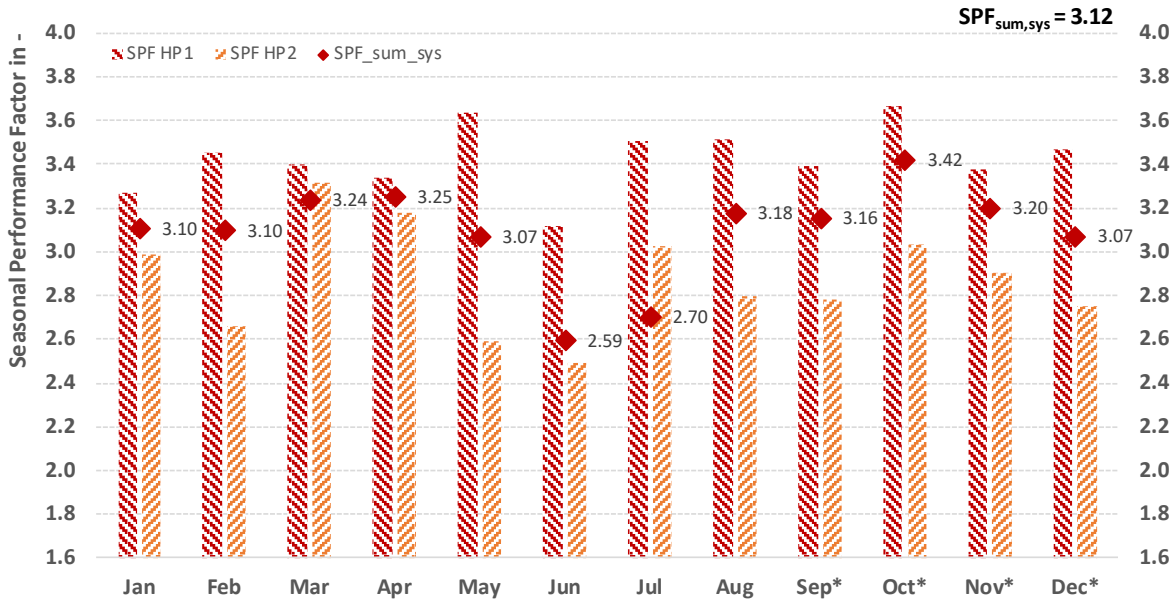


*Figure 4-12: SPF of the two heat pumps and the system (01.01.2018 – 31.12.2018) (*partly missing measurement data)*

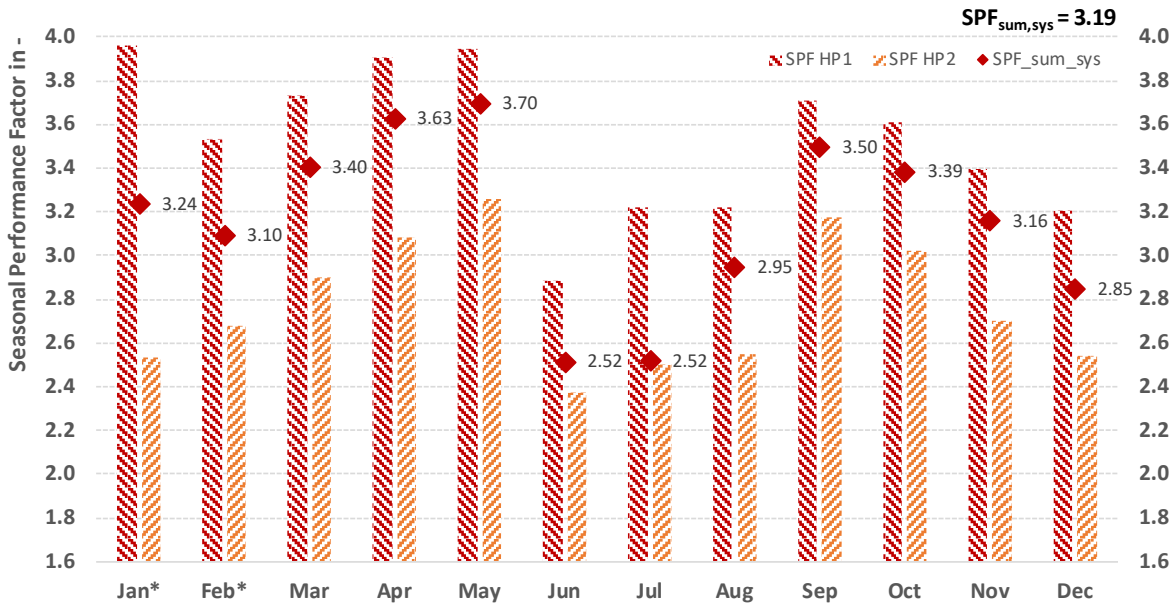


*Figure 4-13: SPF of the two heat pumps and the system (01.01.2019 – 31.12.2019) (*partly missing measurement data)*

Again, the three years show a similar trend of the SPFs. In the periods with high space heating demand (Jan-Apr and Sep-Dec), relatively good performance factors or the HPs (about 3.1 - 3.7) were achieved. Whereby the HP1 shows significantly higher performance factors. In the summer months (Jun - Aug), both HPs achieve significantly lower performance factors (2.5 - 2.8) due to the significantly higher flow temperatures for hot water preparation at similar source temperatures. Here, the efficiency advantage of HP1 over HP2 is evident as well.

Due to the underestimated energy demand (SH & DHW) and the resulting undersized heat sources (ice storage tank and solar air collector), the full performance potential of the analysed system cannot be achieved (for further details see Austrian Task 3.2 report).

# 5 Conclusions

In principle, it can be summarized that the solar ice-storage heat pump system in Weiz required some small modifications during the start-up phase (especially of the control system), but now the system works stable.

One drawback of the realized system is the undersized heat source system for the brine-water heat pumps, due to the underestimation of the energy demand. This results in – timely limited – subcooling of the ice storage tank. Therefore, two additional electric cartridges are operated manually in the two energy storage units (SH & DHW) to cover this heat demand. However, due to the mild winter seasons in the period 2016 – 2020 (+1.3 – 2.7 K above the long-term average), the additional electricity demand is still within an acceptable range of 2 – 4 %. The measured Seasonal Performance Factors taking into consideration the electric direct heating ($SPF_{SumSys}$ acc. to Eq. (2-5)) were 3.1 to 3.2. Of course, these numbers would decrease in case of a significantly colder winter due to a higher share of electricity being used directly (ca. 6 %), as was shown by simulation studies (see Austrian Task 3.2 report).

The undersizing of the heat source system also makes it difficult to make a meaningful comparison of the solar ice-storage heat pump system to classical heat pump systems, such as a brine-to-water heat pump with ground probes or an air-to-water heat pump (see Austrian Task 3.2 report for a comparison with air-to-water heat pump).

In general, the two installed heat pumps in the ice storage system realized here achieve relatively low efficiencies compared to the COPs in the design point. Two points are primarily responsible for this. On the one hand, the heat source side is too small dimensioned, whereby the source temperature in the heating period is clearly below that of a classical brine/water heat pump with horizontal earth collectors. On the other hand, the heat distribution system shows that, in addition to the underestimated energy demand (for heating and especially for domestic hot water preparation), the required temperature level (about 60 °C) for domestic hot water preparation also decreases the efficiency of the heat pumps significantly. Furthermore, the implemented circulation system of the domestic hot water preparation with its return flow into the domestic hot water storage tank leads to a permanent mixing of the water and thus causes a frequent heat pump operation.

The suggestions for improvement, which resulted from the measurements and analyses carried out, especially during the start-up phase, were largely implemented. However, the suggestion to increase the size of the heat source and the realization of direct solar DHW preparation could not be implemented so far, because of the associated costs (see also Austrian Task 3.2 report).

# 6 References

**ABB i-bus®. 2017.** KNX EM/S 3.16.1 Datenblatt. [Online] 2017. [Zitat vom: 06. 04 2017.] http://www.knx-gebaeudesysteme.de/sto_g/English/TECHNICAL_DATA/SINGLE/

EMS_3161_TD_DE_V1-0_2CDC512069D0101.PDF.

**Benkert, St. und Heidt, F. D. 2000.** Abschlussbericht zum Projekt: Validierung des Programms "Graphische Auslegung von ErdwärmeAustauschern GAEA mit Hilfe von Messdaten im Rahmen des Verbundprojekts "Luft-/Erdwärmetauscher" der AG Solar NRW. [Online] Universität-Gesamthochschule Siegen, 02 2000. [Zitat vom: 20. 03 2017.] http://nesa1.uni-siegen.de/softlab/download/abschlussbericht.PDF.

**Diehl Metering. 2017.** Sharky 775 Kompaktenergiezähler. [Online] 2017.

[Zitat vom: 06. 04 2017.] http://www.diehl.com/fileadmin/diehl-metering/pdb/AT_AT_Web/

familie1141551633/SHARKY_775.pdf.

**Elsner Electronic. 2017a.** KNX PY Pyranometer Datenblatt. [Online] 2017.

[Zitat vom: 06. 04 2017.] https://store.casaio.de/media/pdf/38/79/46/KNX_PY_Datenblatt_14

Jul14.pdf.

**Elsner Elektronik 2017b.** KNX TH-UP Thermo-Hygrometer Datenblatt. [Online] 2017. [Zitat vom: 06. 04 2017.] http://www.elsner-elektronik.de/shop/de/fileuploader/

download/download/?d=1&file=custom%2Fupload%2F70366-70368_KNX-TH-UP_Datenblatt_D_23Feb17.pdf.

**Elsner Elektronik. 2017c.** KNX AQS/TH Innenraumsensor Datenblatt. [Online] 2017.

[Zitat vom: 06. 04 2017.] http://www.elsner-elektronik.de/shop/de/fileuploader/download/

download/?d=1&file=custom%2Fupload%2F70161_KNX_AQSTH_Datenblatt_18Apr16.pdf.

**Elsner Elektronik 2017d.** Wetterstation P03/3-RS485-GPS Datenblatt. [Online] 2017. [Zitat vom: 06. 04 2017.] https://www.voltus.de/out/pictures/media/P033-RS485-GPS_Datenblatt_01.pdf.

**Hackl, R. 2016.** Analyse einer realen Eisspeicher - Wärmepumpenanlage mit Solar - Luftkollektoren. Graz : Technische Universität Graz - Institut für Wärmetechnik: Bachelorarbeit, 2016.

**HMI-Master GmbH. 2017.** Homepage [Online] 2017. [Zitat vom: 06. 04 2017.] http://www.hmi-master.at/.

**HOT ICE. 2017.** Photos taken during the project HOT ICE. http://www.innovationszentrum-weiz.at/veranstaltungen-aktuelles/detail/projekt-hot-ice. Weiz.

**Hutter, G. 2016.** E-Mail communication: SG ELIN Weiz, 2016.

**Landis+Gyr. 2017.** T550 Ultraheat. [Online] 2017. [Zitat vom: 06. 04 2017.] http://www.landisgyr.com/webfoo/wp-content/uploads/2013/06/Landis+Gyr-T550-UC50_Projektierungsanleitung.pdf.

**Lerch, W. 2017.** Combined Solar/Heat Pump-System, Draft (unpublished) doctoral thesis, TU Graz - Institute of Thermal Engineering, 2017.

**Minder, S.; Wagner, R.; Mühlebach, M.; Weisskopf, T. 2014.** Eisspeicher-Wärmepumpen-Anlagen mit Sonnenkollektoren. Bern : EnergieSchweiz, 2014.

**Planungsbüro Wolfgang Enthaler GmbH. 2012.** Einreichplan Wohnanlage SG ELIN. Mühlgasse 12 0860 Weiz, 2012.

**Pratter, R. 2017.** Validation of a solar-ice storage-heat pump system and definition of a design guideline, Master Thesis, Graz University of Technology – Institute of Thermal Engineering.

**Pratter, R.; Lerch W.; Heimrath R.; et al. 2017.** Latentwärmenutzung mit Eisspeicher, Wärmepumpe, Solarthermie und PV-Anlage – Systemevaluierung, Systemoptimierung und Dimensionierungsrichtlinie, Project report submitted to the province of Styria, Graz University of Technology – Institute of Thermal Engineering.

**Siemens AG. 2017.** Ultraschall-Wärme- und Kältezähler Datenblatt. [Online] 2017. [Zitat vom: 06. 04 2017.] https://www.downloads.siemens.com/download-center/

Download.aspx?pos=download&fct=getasset&id1=A6V10388513.

**TB Bierbauer GmbH. 2015.** Schautafel HotIce Weiz. 2015. Kontakt: http://www.bierbauer-tb.at/index.php/kontakt.

**TRNSYS_17. 2011.** A Transient System Simulation Program: V17.02.004. Solar Energy Lab. USA : University of Wisconsin - Madison, 2011.

**Viessmann. 2017.** Homepage [Online] 2017. [Zitat vom: 03. 04 2017.] www.viessmann.at.

**Viessmann. 2015.** Montage- und Serviceanleitung VITOCAL 300-G. [Online] 2015

[Zitat vom: 04. 04 2017. http://www.viessmann.com/vires/product_documents/

5724818VSA00003_1.PDF. Allendorf : GmbH, Viessmann Deutschland, 2015.

**Viessman. 2014.** Planungsanleitung Eisspeicher. [Online] 2014.

[Zitat vom: 03. 04 2017.] https://www.alternative-haustechnik.de/media/pdf/48/eb/7b/pa-vie-z013756.pdf. Allendorf : GmbH, Viessmann Deutschland, 2014.

# Appendix - Schematics of the system

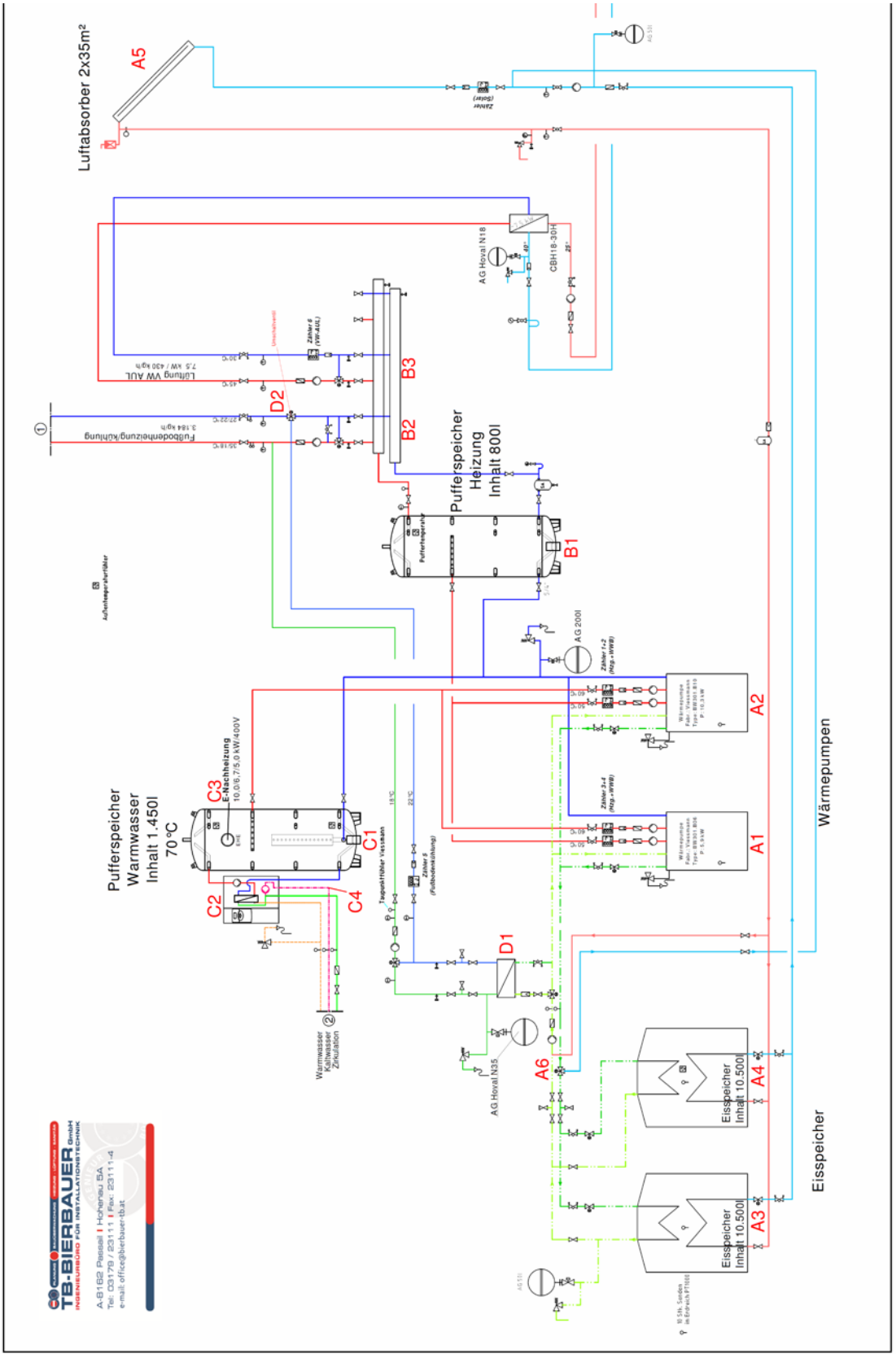


*Figure A- 1: Measurement scheme (TB Bierbauer GmbH, 2015)*

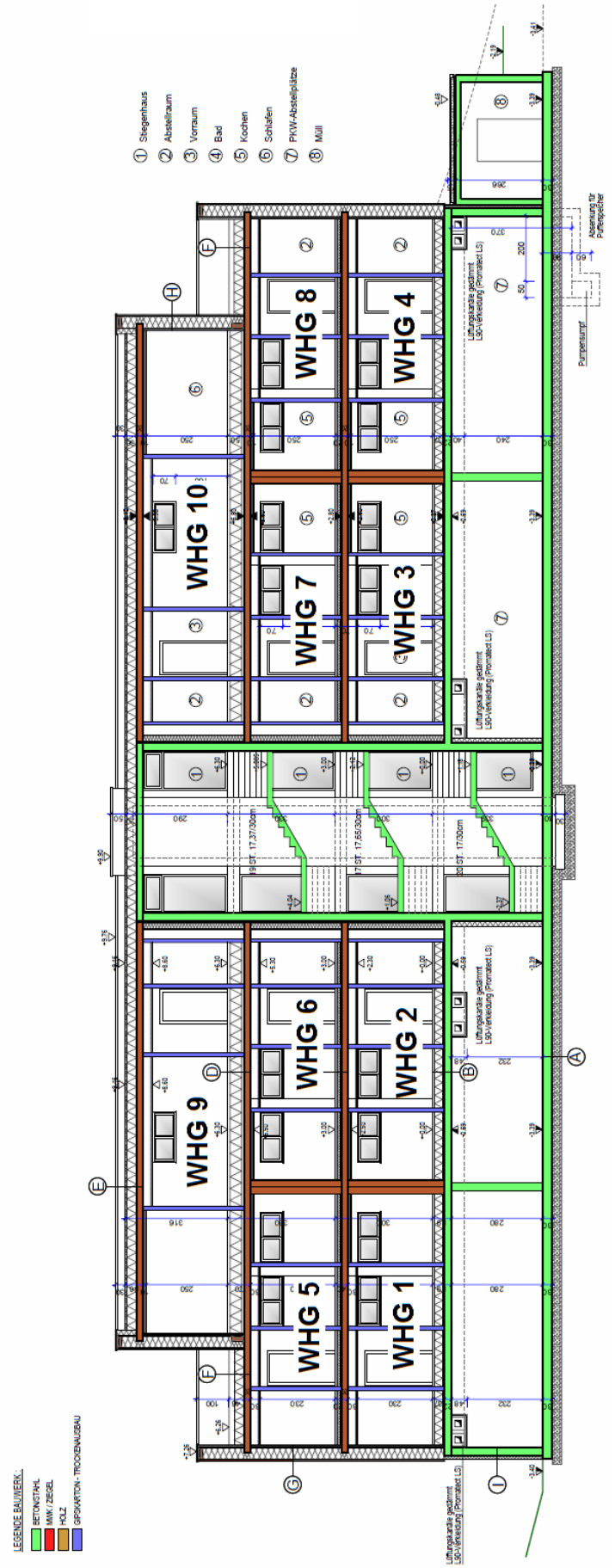


*Figure A- 2: Scheme of the building in Weiz (Planungsbüro Wolfgang Enthaler GmbH, 2012)*